

POLITECNICO DI MILANO

School of Industrial and Information Engineering

Master Degree in Materials Engineering and Nanotechnology

Chemistry, Material and Chemical Engineering Department "Giulio Natta"



**Study of the fracture behavior of
natural rubber and polybutadiene
based compounds:
structure to properties correlation**

Supervisor: Prof. Marta Rink
Co-Supervisor: Prof. Claudia Marano

Master Degree Thesis:
Alessia Bonfanti
N° 782618

Academic Year 2012/2013

Table of contents

Table of contents	1
Figures	3
Tables	8
Abstract	9
Sommario	10
Introduction	11
1. Theoretical background	13
1. RUBBER ELASTICITY THEORY	14
1.1 Thermodynamic approach	14
1.2 Statistical approach	17
1.3 Phenomenological approach	21
2. RUBBER COMPOUNDS.....	24
2.1 Polymers.....	24
2.2 Vulcanization system	26
2.3 Filler.....	28
2.4 Stabilizer system and other ingredients	37
3. FRACTURE IN RUBBER COMPOUNDS.....	37
2. Materials and methods	41
1. MATERIALS.....	41
2. SPECIMEN PREPARATION.....	43
3. TEST METHODS.....	43
3.1 Crosslink density determination.....	43
3.2 Uniaxial tensile tests.....	45

3.3 Dynamic mechanical tests.....	46
3.4 Fracture tests.....	48
3. Results and discussion	55
1. EFFECT OF SULFUR CONTENT	55
1.1 Degree of crosslinking.....	55
1.2 Filler-filler and filler-rubber interactions.....	57
1.3 Strain at the maximum chain extension.....	58
1.4 Ultimate mechanical properties	59
2. EFFECT OF CARBON BLACK CONTENT	63
2.1 Molecular weight.....	63
2.2 Filler-filler and filler-rubber interactions.....	64
2.3 Strain at maximum chain extension.....	67
2.4 Ultimate mechanical behavior.....	68
3. EFFECT OF CARBON BLACK TYPE.....	74
3.1 Degree of crosslinking.....	74
3.2 Filler-filler and filler-rubber interactions.....	75
3.3 Strain at the maximum chain extension.....	77
3.4 Ultimate mechanical properties	77
4. Conclusive remarks	82
References	87

Figures

figure 1: schematization of the empirical and scientific approach to optimize the final rubber properties.....	11
figure 1.1: comparison between rubber and crystalline polymer stress-strain curve (Hertz, 2001)	13
figure 1.2: force at extension of 350 per cent as a function of absolute temperature (Treolar, 2005).....	15
figure 1.3: force at constant length as function of temperature, where elongation is indicated (Treolar, 2005).....	16
figure 1.4: comparison between stress-strain curve of a real rubber and of the theoretical model (Shaw & MacKnight, 2005)	20
figure 1.5: network imperfections: a) physical entanglements, b) closed loop, c) loose ends;.....	21
figure 1.6: Mooney-Rivlin plots for unfilled and filled rubbers (Bokobza, 2001).....	22
figure 1.7: Mooney-Rivlin plots for unfilled and filled natural rubber (a) and styrene-butadiene rubber (b) (Bokobza & Chauvin, 2005).....	23
figure 1.8: cis-1,4 isoprene unit (Mark, Erman, & Eirich, 2005)	25
figure 1.9: possible molecular configurations for butadiene: cis-(1,4) , trans-(1,4) and vinyl-(1,2) (Mark, Erman, & Eirich, 2005).....	25
figure 1.10: three-dimensional rubber network (Mark, Erman, & Eirich, 2005).....	27
figure 1.11: structure of carbon black agglomerate	29
figure 1.12: surface of carbon black primary particle observed by scanning tunneling microscopy (STM) (Mark, Erman, & Eirich, 2005).....	29
figure 1.13: schematic example of occluded rubber for a carbon black aggregate with high structure	30

figure 1.14: comparison of high and low structure carbon black (Dick, 2003)30

figure 1.15: schematic Bueche’s model based on chemical bonds (Mark, Erman, & Eirich, 2005)31

figure 1.16: schematic Dannerberg’s model based on molecular slippage mechanism (Mark, Erman, & Eirich, 2005).....32

figure 1.17: schematic Leblac’s model based on rubber-carbon black physical interaction (Leblanc, 2000).....32

figure 1.18: specific bound rubber as a function of CTAB surface area for different carbon black types at content 50 phr in SBR (Wolff, Wang, & Tan, 1991)33

figure 1.19: bound rubber vs. CTAB surface area for SBR filled with carbon black (Wolff, Wang, & Tan, 1991)34

figure 1.20: effect of carbon black content on compound property (Mark, Erman, & Eirich, 2005)36

figure 1.21: example of video recorded images sequence test of NRBR/S1.5/CB550-35 at displacement rate 50 mm/min.....38

figure 1.22: qualitative physical model of the crack tip during fracture test (Boggio, 2010)39

figure 2.1: dumbbell specimen geometry45

figure 2.2: example of storage modulus-strain curve from dynamic mechanical test and definition of the drop in modulus $\Delta E' = E'0 - E'min$ where $E'0$ is the constant storage modulus at low strain and $E'min$ is the minimum at upturn strain.....47

figure 2.3: four contributions of the storage modulus in the storage modulus-strain curve from dynamic mechanical test: pure rubber network, hydrodynamic effects, filler-rubber interaction and filler network48

figure 2.4: pure shear specimen48

figure 2.5: deformation state in un-notched (a) and notched (b) pure shear specimen.....49

figure 2.6: pure shear groove specimen geometry.....50

figure 2.7: pure shear ungrooved specimen (type I) geometry.....50

figure 2.8: specimen structure before (a) and after (b) vulcanization process.....51

figure 2.9: pure shear ungrooved specimen (type II) geometry51

figure 2.10: example of load-displacement curve where the strain energy at sideways and forward cracks onset.....52

figure 2.11: sketch of subset in the undeformed and deformed image.....53

figure 3.1: molecular weight between two junctions (a) and degree of crosslinking (b) for NR-BR-NRBR/CB550-35 as a function of sulfur content56

figure 3.2: storage modulus drop E' vs strain for NR(a)-BR(b)-NRBR(c)/CB550-3557

figure 3.3: storage modulus at low strain E'_0 and at the minimum E'_{min} from DMA of NR(a)-BR(b)-NRBR(c)/CB550-35 as a function of sulfur amount.....57

figure 3.4: modulus drop from DMA of NR-BR-NRBR/CB550-35 as a function of sulfur amount.....58

figure 3.5: Mooney-Rivlin plot for NR (a), BR (b) and NRBR (c)/CB550-3558

figure 3.6: strain at maximum chain extension for NR-BR-NRBR/CB550-35 as a function of sulfur amount59

figure 3.7: ultimate stress (a) and strain (b) from uniaxial tensile tests as a function of S content.....60

figure 3.8: video frames at sideways and forward cracks onset of NR-BR-NRBR/CB550 as a function of sulfur content61

figure 3.9: J at sideways and forward crack onset of NR-BR-NRBR/CB550-35 as a function of sulfur amount using grooved specimen62

figure 3.10: molecular weight of the chain segments between two junctions (a) and degree of crosslinking (b) of NR-BR-NRBR/S1.5/CB134 as a function of CB content.....63

figure 3.11: storage modulus curve from DMA of NR(a)- BR(b)-NRBR(c)/S1.5/CB134 for different CB content as a function of strain.....64

figure 3.12: storage modulus at low strain (E'_0) and at minimum(E'_{min}) of NR-BR-NRBR/S1.5/CB134 as a function of CB content.....65

figure 3.13: modulus drop of NR-BR-NRBR/S1.5/CB134 as a function of CB content.....66

figure 3.14: normalized storage modulus of NR-BR-NRBR/S1.5/CB134 at CB content as a function of strain66

figure 3.15: Mooney-Rivlin plots of NR, BR and NRBR/S1.5/CB134 with different CB content.....67

figure 3.16: strain at the maximum chain extension of NR-BR-NRBR/S1.5/CB134 as a function of CB content67

figure 3.17: ultimate stress and strain of NR-BR-NRBR/S1.5/CB134 as a function of carbon black content, unfilled NR did not break up to the maximum possible experimental strain.68

figure 3.18: video frames at sideways and forward cracks onset of NR-BR-NRBR/S1.5/CB134 as a function of carbon black content adopting new specimen geometry69

figure 3.19: macroscopic strain, local strain and strain at maximum chain extension at sideways and forward cracks onset of NR (a,b), BR (c,d), NRBR (e,f) S1.5/CB134 as a function of carbon black content70

figure 3.20: J at the sideways and forward cracks onset of NR-BR-NRBR/S1.5/CB134 as a function of carbon black content.....71

figure 3.21: fracture toughness comparison between thesis results (a) and literature data (b)(Cazzoni, Calabrò, Marano, & Rink, 2013).....72

figure 3.22: energy released at forward crack onset of NR/S1.5/CB134-35 and 50 with different combination of batch material and specimen geometry73

figure 3.23: comparison of stress-strain curves of NR/S1.5/CB134-50 and BR/S1.5/CB134-70 characterized by different batch73

figure 3.24: molecular weight of the chain segments (a) and degree of crosslinking (b) of NR-BR-NRBR/S1.5/CB35 as a function of different carbon black types74

figure 3.25: storage modulus curve from DMA of NR(a)- BR(b)-NRBR(c)/S1.5/CB35 as a function of strain.....75

figure 3.26: storage modulus at low strain (E'_0) and at the minimum (E'_{\min}) (a) and modulus drop (b) of NR-BR-NRBR/S1.5/CB35 as a function of different carbon black types76

figure 3.27: normalized storage modulus of NR-BR-NRBR/S1.5/CB35 as a function of carbon black surface area76

figure 3.28: strain at the maximum chain extension of NR-BR-NRBR/S1.5/CB35 as a function of carbon black surface area77

figure 3.29: stress-strain plots from uniaxial tensile tests for NR(a)-BR(b)-NRBR(c) S1.5/CB35 with different CB type78

figure 3.30: ultimate stress (a) and ultimate strain (b) of NR-BR-NRBR/S1.5/CB35 as a function of carbon black surface area78

figure 3.31: video frames at sideways and forward cracks onset of NR-BR-NRBR/S1.5/CB35 as a function of carbon black surface area80

figure 3.32: J at the sideways cracks onset (a) and at forward crack onset (b) of NR-BR-NRBR/S1.5/CB35 as a function of CB surface area81

figure 4.1: average molecular weight between two crosslink points, M_c , as a function of sulfur content (a) and carbon black content (b)82

figure 4.2: E'_{\min} as a function of sulfur content (a) and carbon black content (b)83

figure 4.3: strain at maximum chain extension as a function of sulfur content (a), carbon black content (b) and surface area (c)84

figure 4.4: J at the sideways cracks onset and at forward crack onset of NR, BR, NRBR as a function of sulfur content (a,b), carbon black content (c,d) and surface area (e,f)86

Tables

table 2.1: studied compounds.....	41
table 2.2: properties of carbons black N134 and N550	43

Abstract

The purpose of this thesis work was to study the effect of sulfur (S) content, carbon black (CB) type and carbon black content on the ultimate properties of three different rubber compounds, based on natural rubber, polybutadiene and their 50/50 blend.

First, swelling test, dynamic mechanical analysis and tensile test were carried out to obtain information on physical characteristics of the compounds: crosslink density, filler-filler and filler-rubber interactions and the maximum chain extensibility. Then, ultimate stress and strain from uniaxial tensile tests and the fracture toughness, using notched pure shear specimens and adopting J-integral fracture mechanics approach, were evaluated. Finally, a correlation between the ultimate mechanical properties and the physical characteristics of the compounds was attempted.

The main results obtained are:

- high fracture toughness is achieved when “sideways” cracks, perpendicular to the notch plane, develop before the onset and propagation of “forward” crack along the notch plane;
- “sideways” cracks occurrence depends on crosslink density which can be changed with sulfur and carbon black content. The proper combination of S and CB loadings depends on the particular rubber matrix.
- Even if “sideways” cracks develop, the final toughness depends also on the rubber matrix, crosslink density (varied through S and CB contents) and the type of carbon black.

Sommario

L'obiettivo di questa tesi è stato quello di studiare l'effetto del contenuto di zolfo (S), del tipo e del contenuto di nerofumo (carbon black CB) sulle proprietà ultime di tre diverse gomme: gomma naturale, polybutadiene e la miscela 50/50 delle due.

Innanzitutto, sono state determinate le caratteristiche fisiche degli elastomeri. Attraverso test di rigonfiamento, analisi dinamico-meccaniche e test di trazione uni assiale è stato possibile ottenere informazioni riguardanti la densità di reticolazione, interazione filler-filler, filler-gomma e la deformazione in corrispondenza della massima estensione della catena. In seguito, è stato analizzato il comportamento ultimo dei materiali, conducendo test di trazione, mentre la tenacità a frattura è stata determinata basandosi sulla definizione d integrale J utilizzando provini con geometria pure shear. Nella fase finale del lavoro si è cercato di correlare le proprietà meccaniche ultime con le caratteristiche fisiche del composto.

I risultati ottenuti sono:

- La formazione e sviluppo di cricche, che si propagano perpendicolarmente al piano dell'intaglio ("sideways cracks") prima che si sviluppi la cricca in direzione del piano dell'intaglio (forward crack), mostrano un aumento della tenacità a frattura.
- La condizione per l'innesco e la propagazione delle "sideways cracks" dipende dal grado di reticolazione, che varia in funzione del contenuto di zolfo e nerofumo. La corretta combinazione di quantità di S and CB è legata al tipo di matrice.
- Anche se le "sideways cracks" si sviluppano, la tenacità finale dipende dalla matrice di gomma, dalla densità di reticolazione (attraverso la variazione di S and CB) e dal tipo di carbon black.

Introduction

Rubbers are widely used due to their main property: high elasticity shown at large level of strains. In fact these materials are able to reach high deformation and to recover completely the initial shape and dimensions. These characteristics derive from the three-dimensional molecular networks, obtained through a crosslinking process that generates chemical bonds among the polymeric chains.

The largest application is in the tire industry, where the main requirements are rolling resistance, grip and wear resistance related to energy consumption, safety and durability. The optimization of these properties and other requirements, such as resistance to oxygen and chemical agents are obtained selecting the proper rubber and compounding it with other ingredients, such as crosslinking agents and reinforcing fillers.

From a general point of view, to achieve the good fracture behavior of these materials two different approaches can be adopted (figure 1).

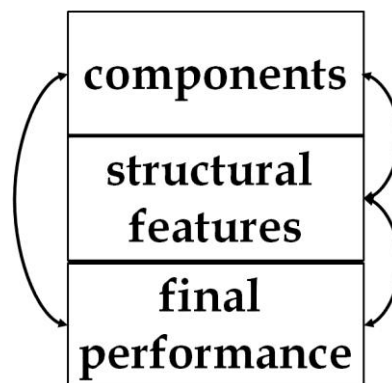


figure 1: schematization of the empirical and scientific approach to optimize the final rubber properties

One is an empirical method: the components of the rubber compounds (in terms of contents and types of ingredients) are directly correlated to their final performance. The second one is a more scientific approach. It is characterized by a mid-step analysis, that consists on the evaluation of the structural features, determined by the

components of the rubber compounds. Thus, this method correlates the ingredients to the physic structure, which in turn is correlated to the fracture performance.

An attempt to apply the more scientific approach is made in this thesis project to study the effects of the content of sulfur, the amount and the type of carbon black on three different rubber matrices. The rubbers considered are industrial products widely used in the field of tires: natural rubber, which guarantees strength, polybutadiene, which provides abrasion resistance, and finally 50-50 blend of them, that improves fatigue and crack growth resistance. The presence of reinforcing filler, like carbon black, in the compounds enhances the strength, abrasion resistance and the stiffness.

The correlation between the components of the compounds and their physical structure was found analyzing the degree of crosslinking, the filler-filler and filler-rubber interactions and the orientability of the molecular chains performing swelling tests, dynamic mechanical analysis and uniaxial tensile tests. To evaluate the mechanical behavior the ultimate stress and strain and fracture toughness were determined. The compounds toughness was measured carrying out pure shear tests using a suitable specimen geometry in order to study better the fracture phenomenology. It was applied fracture mechanics, basing on energy approach.

This thesis work is organized in three main chapters.

The first one introduces briefly the field of rubbers, explaining the theoretical basis of the elastic phenomena, the different “ingredients” of the rubber compounds, focusing in details on the sulfur and carbon black properties, and fracture phenomenology, observed in filled rubbers.

The second chapter shows the materials analyzed and explains the overall performed tests.

The last chapter concerns the results obtained and the comments about them.

1.Theoretical background

The success of rubbers is directly linked to the high elasticity shown up to large deformations, that guarantees the ability to recover completely the shape and the initial dimensions. The requirements necessary to define a rubber are the presence of long-chain molecules, weak secondary forces between the polymeric chains and the formation of a coherent network structure, characterized by chemical bonds between macromolecules. When the compound is stretched, the long polymeric chains are imagined to be free to rotate around the bound along the main chain, thus they are able to assume different conformations. To guarantee their motion it is important that the neighboring macromolecules don't obstacle each other, i. e. the forces among them should be weak. At the same time the polymeric chains must not slip independently. Some cross-links or junction points are therefore introduced, whose number should be such as to avoid that rubbers behave like a liquid and at the same time do not interfere with the free movement of macromolecules.

To have a general idea about their behavior, an elastomers, which is amorphous, is compared to a crystalline polymer: it appears soft, characterized by low modulus, highly elastic and highly deformable.

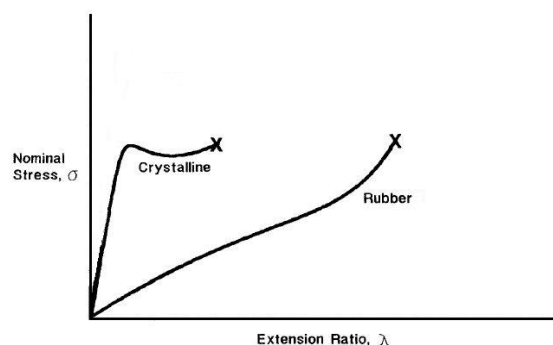


figure 1.1: comparison between rubber and crystalline polymer stress-strain curve (Hertz, 2001)

1. RUBBER ELASTICITY THEORY

The main property of rubbers is the elasticity, that is linked to their ability to stress and to extend their length several times and to recover completely the initial dimensions with small or without residual deformations. This typical behavior distinguishes this kind of material from other ones, like crystalline solids, which cannot deform widely, or ductile materials, that can reach high value of strain but are not able to return to their original length removing the input stress.

The rubber elasticity is an interesting and controversial topic that was extensively discussed in the past. Several approaches are adopted studying and describing the same phenomena from different points of view. The thermodynamic approach is the classical one, in which attention is focused on the macroscopic behavior. The statistical mechanics is another treatment that investigates the molecular structure of rubber, where the flexibility of the polymer chain is described in a statistical way. The last one is a phenomenological approach, which is not based on molecular concepts but only on mathematical reasoning. Its aim is to obtain a general and convenient formulation to describe the properties, for example it permits to describe the elasticity in a three dimensional network up to large deformations.

All these three approaches together permit a more complete description of rubberlike behavior. In fact, the thermodynamic approach, performed in a simple way, allows to lay solid basis for the development of a statistical theory and for understanding the physical meaning.

1.1 Thermodynamic approach

This approach on the elasticity of rubber concerns an energetic analysis, also linked to the disorder state of the system. After the deformation under constant temperature (T) and pressure (P), the restoring force (f) is given by two contributions; one enthalpic (H) and one entropic (S):

$$f = \left(\frac{\partial H}{\partial L} \right)_{T,P} - T \left(\frac{\partial S}{\partial L} \right)_{T,P}$$

The rubber behavior is examined using the kinetic theory, that attributes the elasticity to the variations in conformations of the long polymeric chains, which move from unstrained to strained state. The main consequence is that only the configurational entropy of the system changes, while the internal energy remains constant. Under these conditions, the stretching force for a given state of strain should be proportional to the absolute temperature.

$$f \sim -T \left(\frac{\partial S}{\partial L} \right)_{T,P} \sim T \left(\frac{\partial f}{\partial T} \right)_{P,L}$$

For low strain the experimental data show an anomalous behavior, because at constant level of deformation increasing the temperature the restoring force decreases, reaches a minimum, after which it increases as expected theoretically (figure 1.2). The reason is related to the contribution of the thermal expansivity of the unstrained rubber, whose effect dominates more at small strain: an increase of temperature at constant length causes a reduction of strain or relative extension determining a reduction of the applied force.

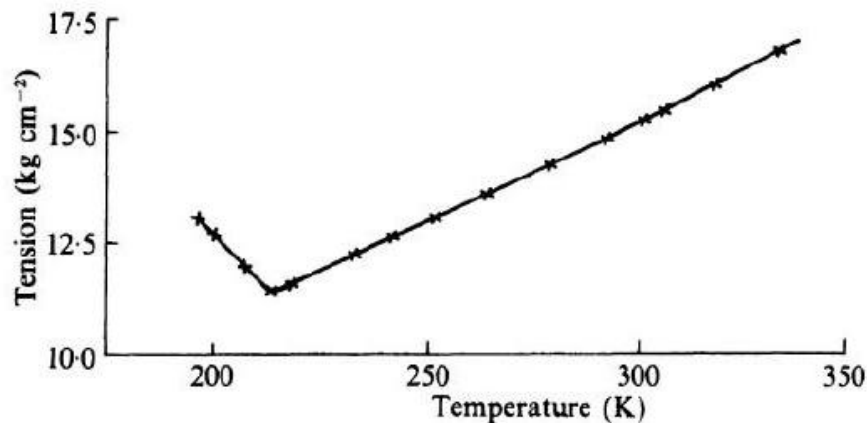


figure 1.2: force at extension of 350 per cent as a function of absolute temperature (Treolar, 2005)

In the same way, varying the deformation level stress-temperature curves show different slopes (figure 1.3).

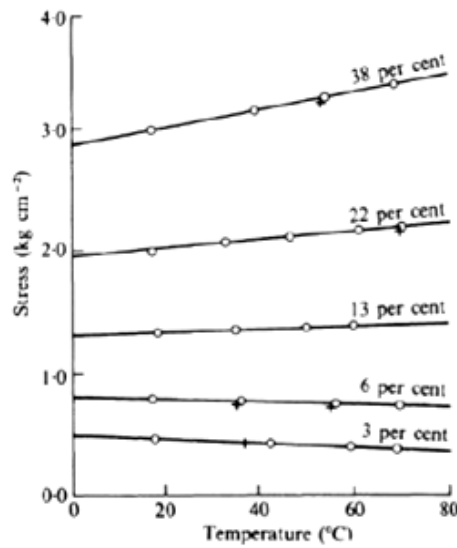


figure 1.3: force at constant length as function of temperature, where elongation is indicated (Treolar, 2005)

This phenomenon is called thermoelastic inversion, that can be understood analyzing the variation of restoring force (f) as a function of temperature (T)

$$\left(\frac{\partial f}{\partial T}\right)_{P,L} = \frac{f - (\partial H/\partial L)_{T,P}}{T}$$

where dH is the infinitesimal variation of enthalpy due to the deformation dL imposed at constant temperature and pressure.

The negative slope appears at low strains when $(\partial H/\partial L)_{T,P} > f$, that means that the contribution of internal energy is more important than the elastic phenomena.

Increasing the level of deformation the slope turns positive, $(\partial H/\partial L)_{T,P} < f$, so the enthalpic component becomes less important, until at high levels of stress it can be neglected. Under this condition, it is possible to assume that the elastic response is completely governed by the decrease of entropy resulting from the deformation of the chains.

This analysis is too restrictive because at very high strain the contribution of enthalpy should assume again a certain importance due to the increase of limitations of the chains extension and mobility, as well as the onset of crystallization. This can be explained considering that the variation of enthalpy is

influenced by two contributions: one depends on volume and the other on the deformation of the material at constant volume. This second part cannot be related to the molecular nature of the elastomers, thus it could be probably function of intramolecular energy effects.

1.2 Statistical approach

The conclusion derived from the thermodynamic approach makes the basis for the statistical treatment: the proportionality between the stress of a deformed elastomer, linked to the restoring force, and the temperature describes the behavior of a ideal gas. So the assumption for the molecular theory concerns the association of an ideal elastomers to an ideal gas.

An ideal gas is a collection of point masses, which are randomly disposed and move independently each other. At constant temperature, the restoring force depends only on the state of disorder of the system. In fact, the internal energy is independent of the volume, while the entropy is composed by two contributions: one associated to heat capacity and independent of the volume and the other one linked to the configurational entropy, which is a function of the volume.

An ideal elastomer is a collection of long, flexible and volumeless chains, that rearrange continually reaching different conformations, equally probable. An important point is the presence of chemical junctions between polymeric chains introduced to avoid the flow of macromolecules. As for the ideal gas, it is possible to do the same considerations about the thermodynamic factors: internal energy does not depend on the elongation, so the stress or restoring force is attributed only to the configurational entropy and this is due only to the conformational changes arising from the rotations about single bonds in the chain backbone.

The analysis of the elasticity of rubber with the statistical approach is based on four simplifications:

- 1) The internal energy of the system does not depend on the conformations of the single chains, but only the entropic term is influenced.

- 2) The single chain is freely jointed and volumeless, this means that it obeys to Gaussian statistics, thus the number of available conformations is given by the Gaussian distribution function.
- 3) The total number of conformations is the product of the number of conformations of the individual network chains.
- 4) Crosslink junctions are fixed at their mean positions, and during the deformation they transform affinely. The assumption of affine deformation means that the microscopic strain of the chains is related to the macroscopic strain of the elastomers sample.

These assumptions appears too restrictive for a realistic description of rubbers, in particular about the definition of the single chain and of crosslink points.

In a real elastomer, it is not possible to assume that the network chains in the unstrained state have the same distribution of conformations of freely orienting random chains, because during the vulcanization process some of them can be partially strained, so the end-to-end distance of isolated chain is different to the end-to-end distance of the chain in the network.

The idea of volumeless, which means there is no material existence, defines the polymeric chain as "phantom chain". The individual macromolecules and the crosslink points may pass through one another in order to readjust reaching the lowest level of energy in the strained state. Under this condition, the mean position of crosslink points is consistent with affine deformation, but around this point some fluctuations of the junctions are allowed and are not affected by the macroscopic state of deformation. This means that the distribution function, characterizing the position of crosslinks, cannot be simply correlated to that in undeformed network with an affine transformation.

The assumptions regarding the position and transformation of crosslink points in the real networks are too restrictive. During the deformation the junctions would be expected to move and pass one another, not properly in an affine mode, this means that the relative position of each chemical crosslink can change, so the neighborhood varies.

These last two points define two extreme behaviors about elastomeric material. So it is possible to imagine that a real rubber probably shows an intermediate performance, because not all crosslink points move affinely and the steric interactions are strong enough to prevent phantom approximation.

The equation of state for rubber elasticity obtained with a statistical treatment should be the expression of the total elastic restoring force as a function of deformation. To be able to describe the behavior of elastomers under different state of strain, a more general formula is derived, where the nominal stress, instead to the total force $f(\sigma = \frac{f}{A_0})$, is related to the deformation:

$$\sigma = N_0 RT \frac{\overline{r_0^2}}{r_f^2} \left(\lambda - \frac{V}{V_0 \lambda^2} \right)$$

where

- $N_0 = N/V_0$ defines the number of network chains per unit volume of undeformed sample. It can be also used as the number of moles of network chains per unit volume (mol/m³).
- R = gas constant (8.315 Pa m³/mol K).
- T = temperature expressed in Kelvin.
- $\overline{r_0^2}$ = mean square end-to-end distance of the chain in the network.
- r_f^2 = mean square end-to-end distance of the isolated chain.
- $\frac{V}{V_0}$ = is the ratio of the volume in the unstrained and strained state. Its value is very near to the unity, so $\frac{V}{V_0} \sim 1$
- λ = extension ratio, expressed $\lambda = \frac{l}{l_0} = \frac{l_0 + \Delta l}{l_0} = 1 + \varepsilon$

Based on the definition of the tensile modulus as the limit for very small strain of the ratio of true stress and deformation, it could be derived that the shear modulus G is given by:

$$G = N_0 RT \frac{\overline{r_0^2}}{r_f^2}$$

So the equation of state can assume this simple form $\sigma = G \left(\lambda - \frac{1}{\lambda^2} \right)$

From a theoretical point of view, the equation seems to be able to predict the correct behavior because the stress, linked to the elastic force, is directly proportional to the temperature and to the total number of chains in the network, as experimentally observed. Comparing the theoretical and the experimental stress-strain curves (figure 1.4), for low level of deformation ($\epsilon < 50\%$ or $\lambda < 1.5$), the model foresees in a good way the real behavior of rubbers, while at high strain it is not able to predict the increase of modulus.

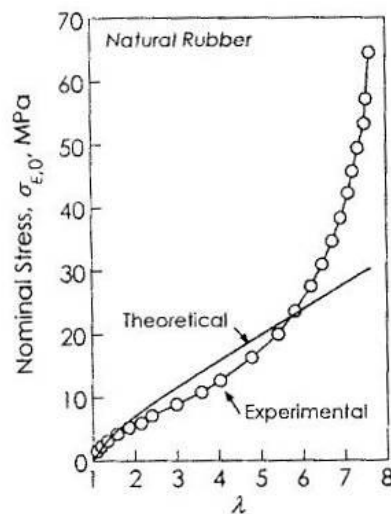


figure 1.4: comparison between stress-strain curve of a real rubber and of the theoretical model (Shaw & MacKnight, 2005)

Some assumptions of the theory become too restrictive and also some other aspects are neglected, for example:

- The Gaussian statistic is too rough for high deformations.
- The hypothesis of affine transformation is no more valid at high strain.
- Stereoregular polymers can crystallize under strain.
- The presence of network imperfections must be considered. In fact the real structure is far from the idealized for tetra-functional crosslinking, where the number of chains is exactly twice the number of junction points and every chain will contribute equally to the network elasticity.

Three types of network defect are identified (figure 1.5):

- a) physical entanglements between chains, that have an effect comparable to the chemical cross-linkage, increasing the modulus;
- b) closed loop, derived from the linkage of two points on a single chain, which does not influence the elasticity of the system;
- c) loose ends, consisting of chains that are connected to the network at only one end, so also in this case there is no contribution to elasticity.

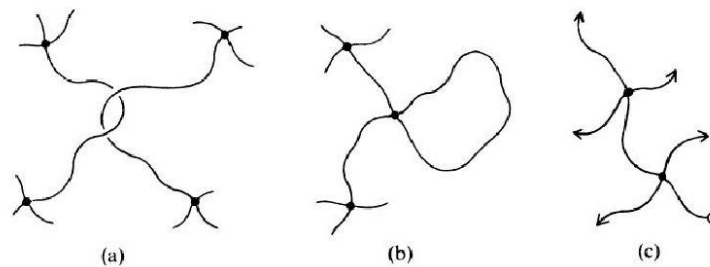


figure 1.5: network imperfections: a) physical entanglements, b) closed loop, c) loose ends; where ● crosslinkages, ○ chain termination (Treolar, 2005)

1.3 Phenomenological approach

The statistical theory does not give a complete description of the stress-strain behavior of rubberlike material, due to many rather drastic simplifying assumptions. So to formulate a relation able to describe the elastomers' behavior over a larger range of strain, a phenomenological treatment is adopted. It is based on the observed behavior and on mathematical concepts, using continuum mechanics.

Firstly, on the assumption of isotropy and constant volume, the problem was focused on the determination of an expression for the elastic stored energy as a consequence of the level of strain reached. In the following this result was developed deducing the nominal stress and the equation obtained is known as Mooney-Rivlin equation:

$$\sigma = 2 \left(C_1 + \frac{C_2}{\lambda} \right) \left(\lambda - \frac{1}{\lambda^2} \right)$$

Where λ is the extension ratio, C_1 and C_2 are material constants: C_1 depends on temperature and the density of crosslinking, while C_2 provides the deviation from the ideal Gaussian behavior.

Using this equation, it is possible to obtain the “reduced stress” (σ^*)

$$\sigma^* = \frac{\sigma}{\left(\lambda - \frac{1}{\lambda^2}\right)} = 2 \left(C_1 + \frac{C_2}{\lambda} \right)$$

Reduced stress is plotted as a function of the inverse of the extension ratio.

Each elastomer shows a proper behavior: for example an ideal rubber has a constant trend, due to the constant restoring force (thus this means C_2 is equal to zero in reduced stress equation), while a real rubber deviates from this behavior.

Going into details as reported by Bokobza (Bokobza, 2001), a vulcanized unfilled real rubber shows a linear decreasing trend at large deformation, while a vulcanized filled rubber determines also deviations from the linear trend at the extremes of deformation. In the following figure 1.6, at low strain, the reduction of the modulus due to the filler network breakage (Payne effect) can be observed. At high level of deformation an increase of stress is usually shown due to the limited chain extensibility: indeed the upturn corresponds to the minimum of the Mooney-Rivlin curve and it should represent where the chain segments between two crosslink points reach their maximum extension. The unfilled material is able to reach this point too, but for higher deformations.

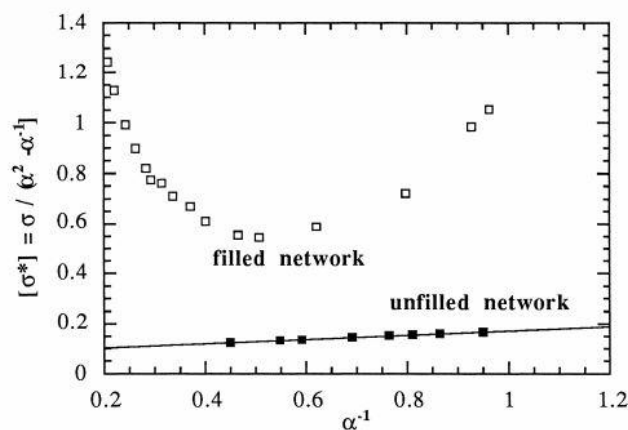


figure 1.6: Mooney-Rivlin plots for unfilled and filled rubbers (Bokobza, 2001)

The choice of the polymer matrix influences strongly the behavior at high deformation, in fact some materials begin to crystallize under strain: this phenomena is known as strain induced crystallization (SIC).

Bokobza and Chauvin (Bokobza & Chauvin, 2005) compare two rubbers: natural rubber, which is always able to crystallize and styrene-butadiene rubber, that is not able to form crystallites. It is interesting consider that also unvulcanized natural rubber is able to crystallize due to the presence of pseudo network, called also naturally occurring network, generated by the interaction of polymeric chains with the non-rubber components (as proteins, phospholipids, metal ions) (Amnuaypornsi, Toki, & Hsiao, 2012)

In fact, (figure 1.7) natural rubber, independently to the presence and to the amount of reinforcing fillers, always shows the increase of the reduced stress, thanks to its high stereoregularity. For unfilled and low filled (10 phr) SBR no increasing stress is verified, while for high content its growth reveals the presence of filler and rubber. Moreover they study also the influence of different degree of crosslinking: the deformation at which the modulus upturns, decreases with the increase of filler content.

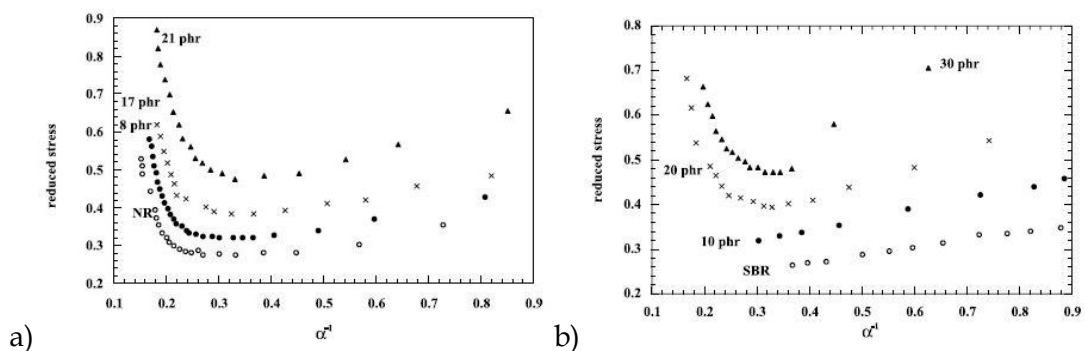


figure 1.7: Mooney-Rivlin plots for unfilled and filled natural rubber (a) and styrene-butadiene rubber (b) (Bokobza & Chauvin, 2005)

2. RUBBER COMPOUNDS

Elastomers or rubbers are generally not constituted only by raw materials. They are employed as compounds, in order to optimize the properties of the neat rubber for the required performances and the specific applications.

The main components of a rubber compound (Mark, Erman, & Eirich, 2005) are:

- 1) Polymers;
- 2) Vulcanization system;
- 3) Filler;
- 4) Stabilizer system;
- 5) Other ingredients.

In this thesis the effect of three of these ingredients were studied: the type of polymer, crosslinking agents (responsible of the formation of a network) and the reinforcing fillers.

In the following, attention will be focused on the points interesting, already mentioned.

2.1 Polymers

Three different polymers are considered polyisoprene, polybutadiene and the 50-50 blend of them.

They are "diene" rubbers, i. e. the monomeric units contain double bonds and make them rather susceptible to the attack of oxygen and of ozone. At the same time, the unsaturated bonds guarantee the chemical reactivity with sulphur in order to create chemical crosslinks that are responsible of the three-dimensional network.

NATURAL RUBBER

Natural rubber is produced from the latex of the Hevea Brasiliensis tree: it is present in form of small particles dispersed in the latex. The molecular weight is in the range of 10^4 - 10^7 g/mol.

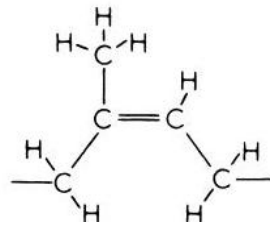


figure 1.8: cis-1,4 isoprene unit (Mark, Erman, & Eirich, 2005)

Natural rubber is defined by hydrocarbon polymeric chains $(C_5H_8)_n$ and its structure is completely cis-1,4-polyisoprene (figure 1.8), except for the chain ends. The configuration is stereoregular and therefore the polymer may crystallize. In particular the maximum crystallization rate is at $-25\text{ }^\circ\text{C}$ (Hamed, Materials and Compounds, 2001).

Considering that the glass transition temperature of this material is about $-70\text{ }^\circ\text{C}$, at room temperature natural rubber is an amorphous polymer, whose macromolecules show a random coil conformation, that means the entropy level is very high. This state of disorder tends to decrease when the sample is deformed: the macromolecules align in the direction of applied load and the material crystallizes. This gives rise to a an increase of resistance. An important role is played by the vulcanization process, that introduces chemical crosslinking points among the macromolecules in order to avoid viscous flow.

The main properties of natural rubber are: oil resistance, low gas permeability, improvement of wet grip and rolling resistance, coupled with high strength.

POLYBUTADIENE

Polybutadiene is characterized by hydrocarbon structure $(C_4H_6)_n$. The monomeric unit can arrange in three different molecular configurations (figure 1.9): cis-(1,4), trans-(1,4) and vinyl-(1,2) or (3,4).

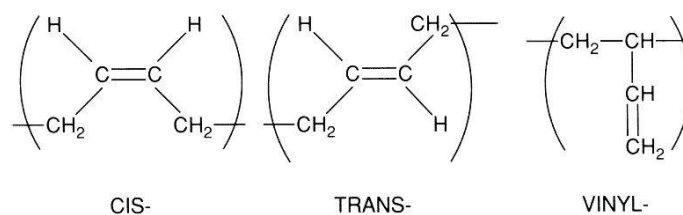


figure 1.9: possible molecular configurations for butadiene: cis-(1,4), trans-(1,4) and vinyl-(1,2) (Mark, Erman, & Eirich, 2005)

The relative content of each isomers in the final product influences the material's performance (Mark, Erman, & Eirich, 2005). In particular with regard to tyres field, it may change properties, like abrasion and wear resistance, rolling resistance, wet grip. There are some methods to obtain this rubber that generate polymers with different percentage of the three molecular configurations. In tyre industry polybutadiene with high cis-content structure is widely used.

As natural rubber, at room temperature polybutadiene is an amorphous polymer. Its glass transition temperature changes as a function of the amount of vinyl: with low content it is about -100 °C, (Hamed, Materials and Compounds, 2001).

50/50 NR/BR BLEND

The blend of natural rubber and polybutadiene is considered to be heterogeneous characterized by two-phase structure, although the detailed morphology is not still well known.

The presence of other ingredients, as carbon black fillers, zinc oxide or proteins, favors the heterogeneity, because the different affinity of the polymers with them could modify the distribution (Sircar, Lamond, & Pinter, 1973). In fact not only the relative compatibility of the elastomers but also the processing conditions (as the sequence of ingredients addition (Sircar, Lamond, & Pinter, 1973) and the amount of mixing (Walters & Keyte, 1965)) can affect the phase zone-size. Walters and Keyte determine that the physical properties are not affected by the dimension of heterogeneity, but by the non uniform distribution of the other compounding ingredients between the polymers.

Nevertheless this blend is widely used in the tyre industry since for specific formulations it is able to improve fatigue and crack growth resistance.

2.2 Vulcanization system

A polymer above its glass transition temperature is a high molecular weight liquid. The long polymeric chains are entangled and under an applied stress they disentangle leading to viscous flow. In this condition, the polymer shows low elasticity and low strength. Therefore it is necessary to create chemical junctions (crosslinks) between adjacent polymer chains: in this way the material is

transformed from a viscous liquid to an elastic solid, i. e. if stressed up to high strains, it shows no permanent deformation after the removal of the load. The main disadvantage of this process is its irreversibility: so after chemical reactions occur, the component has to assume the desired shape.

In the rubber industry sulfur and peroxides are the most common as crosslinking agents, in particular the materials studied in this thesis work were all characterized by the presence of the first one.

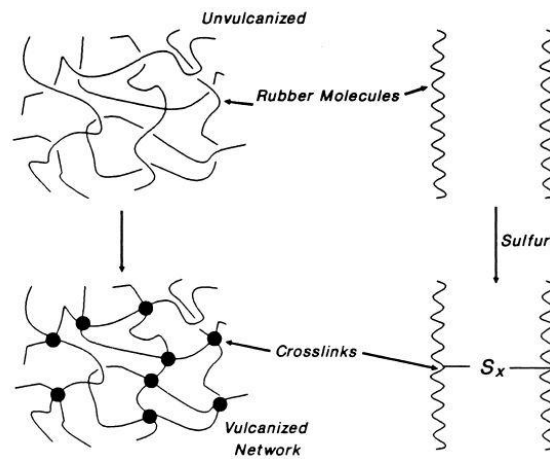


figure 1.10: three-dimensional rubber network (Mark, Erman, & Eirich, 2005)

Generally, sulfur is used on combination with other ingredients, which control the crosslinking reaction: activators and accelerators.

During the thermal process sulfur is able to react with the double bonds of the polymeric chains, forming chemical crosslinks (figure 1.10). Thus it has great influence on the formation and type of the three-dimensional rubber network. The amount of vulcanizing agents is important because it defines the degree of crosslinking, on which the behavior of rubber depends. It must be high enough to prevent by viscous flow, but not too high in order to have good mechanical properties. Further the type of crosslinks plays an important role: it depends on sulfur level, accelerator type, accelerator/sulfur ratio and cure time. Usually, it is possible to recognize two different types of sulfur linkages that depend on the sulfur and accelerators content and on the vulcanization time: monosulfidic (consisting on carbon-sulfur bond) and polysulfidic (where the vulcanizing agent links to other vulcanizing agent forming S-S bonds) (Hamed, Materials and

Compounds, 2001). For example, high accelerator/sulfur ratio and longer cure time increase the probability to create monosulfidic bonds despite of polysulfidic ones. The greater stability of C-S bonds compared to S-S bonds determines that rubbers with more monosulfidic crosslinks have better heat stability, than those with polysulfidic links. On the other hand, compounds containing a high amount of polysulfidic crosslinks are characterized by greater tensile strength and fatigue crack resistance.

2.3 Filler

The presence of fillers in the rubbers is very important, because they are able to improve wear resistance, strength and elastic modulus. In general nonreinforcing and reinforcing fillers can be adopted (Mark, Erman, & Eirich, 2005). The first kind is not used in rubber field: no inert ingredients are added to reduce the final cost. The second ones are employed because they are able to increase the stiffness of elastomers without reducing neither their strength nor their elastic properties. A great variety of fillers can be used in rubber compounds: carbon black, zinc oxide, carbonates and silicates of calcium and magnesium.

The attention is focused on carbon black, because the rubbers considered in this thesis work are filled with these reinforcing particles.

Carbon black is the most employed filler in the tyre industry. The final strength and the properties depend on its content and its features. There is a great number of carbon black types, the relevant choice is related to the product performance.

2.3.1 MORPHOLOGY AND STRUCTURE OF CARBON BLACK

Carbon black (figure 1.11) presents itself as an agglomerate, but when it is mixed with the rubber and the other ingredients, it breaks up and forms aggregates, that are considered to be the reinforcing objects.

These aggregates are weakly bound to each other and this guarantees an easy distribution during mixing. Their structure is characterized by primary spherical particles, that are partially fused together and are arranged irregularly with a branched shape. The main feature of an aggregate is the impossibility to divide it

into primary particles: this explains why it must be considered as the reinforcing object.

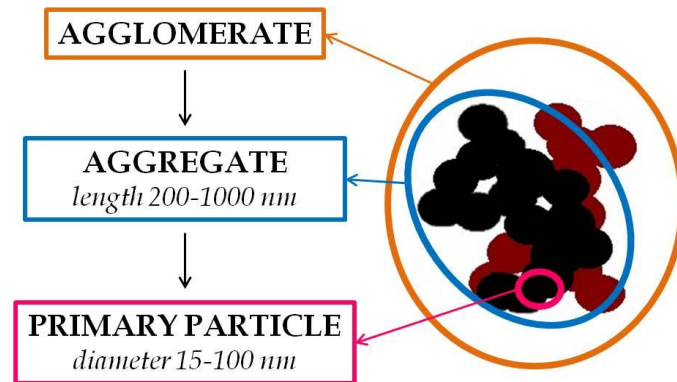


figure 1.11: structure of carbon black agglomerate

The size of the particles is an important property that can be used as an index of the surface interaction between the polymeric and the reinforcing phase: the smaller the particles, higher the interaction interface. Using scanning tunneling microscopy (STM), their surface appears as a composed structure formed by overlapping graphitic layers (figure 1.12) (Mark, Erman, & Eirich, 2005).

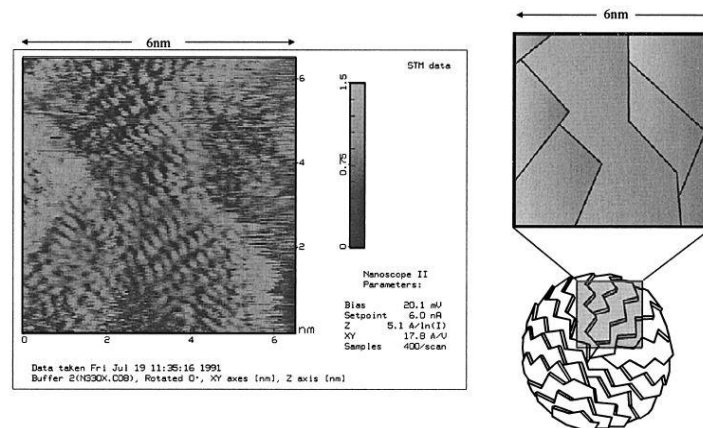


figure 1.12: surface of carbon black primary particle observed by scanning tunneling microscopy (STM) (Mark, Erman, & Eirich, 2005)

It is to be noted that part of the elastomer may be trapped inside the aggregate structure (occluded rubber) (figure 1.13). When the irregularity in shape is high, the aggregate void volume is larger, so more occluded rubber is present. This trapped polymer is unable to deform and behaves like filler.



figure 1.13: schematic example of occluded rubber for a carbon black aggregate with high structure

2.3.2 FILLER DISPERSION IN THE RUBBER MATRIX

The mechanical behavior of rubber compounds depends also on fillers dispersion. To guarantee it, a Banbury mixer is generally employed, which firstly distributes the agglomerates in the pure polymer, which break-up forming aggregates. Filler dispersability and therefore its dispersion depend on aggregate surface area, on structure (referred to the way how carbon black is constructed) and surface energy, which difference between carbon black and the polymeric matrix defines the strength of interactions of reinforcement and matrix (Dick, 2003).

An higher dispersion is guaranteed by small particles, high aggregates structure and similar surface energies of rubber and filler. In details, the small primary particles determine large surface extension so more rubber-filler interaction, while higher structure, that means more “open” (figure 1.14) suggests less tightly packed carbon black, characterized by a lower number of contact with the neighbors and so lower interaggregate attractive forces.

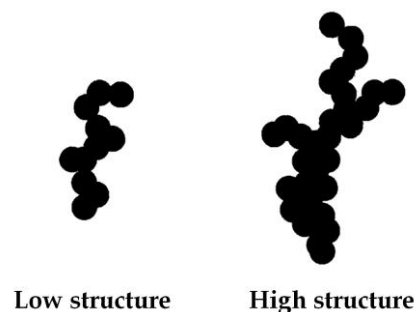


figure 1.14: comparison of high and low structure carbon black (Dick, 2003)

Nevertheless in the dry state, so before mixing, the high surface area and the low structure have a negative influence on the filler dispersion: in fact small aggregates interact more with their neighbors and the low structure defines carbon black with more compact particles.

One important aspect to consider is the impossibility to obtain a distribution of same dimensions aggregates. Indeed, on one side the dispersion appears incomplete because some agglomerates keep their structure, so the size of reinforcing object increases; on the other side the high levels of shear stress can cause the breakage of the agglomerates, so the size of reinforcing object is lower than what it is expected.

2.3.3 RUBBER-CARBON BLACK INTERACTION

The type of interaction between rubber and carbon black has been widely studied.

In the past, Bueche (Mark, Erman, & Eirich, 2005) supposed that the carbon black reinforcement depended on the strong covalent bonds obtained by the reactions of its acidic groups with hydrocarbon chain. The polymeric segments between two fillers are characterized by different length, so during stretching when the shortest reaches its maximum extension, it breaks and the stress is shared by the other bridging chains (figure 1.15).

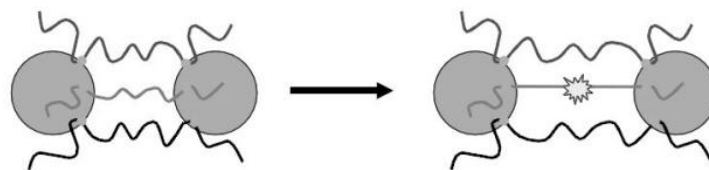


figure 1.15: schematic Bueche's model based on chemical bonds (Mark, Erman, & Eirich, 2005)

Later it was demonstrated that this chemical interaction was not responsible for reinforcement. A new mechanism, called "molecular slippage", was introduced by Dannerberg as reported in *The science and technology of rubber* (Mark, Erman, & Eirich, 2005). Due to the different levels of surface energy between carbon black and rubber, a small part of macromolecules is strongly adsorbed on the filler surface. The low energy of this phenomenon and the reversibility permits a continuous change of elastomer-filler contacts and so the possibility to have its homogenization

of bridging segments length (figure 1.16). In this case near the interface the mobility of polymeric chains is reduced.

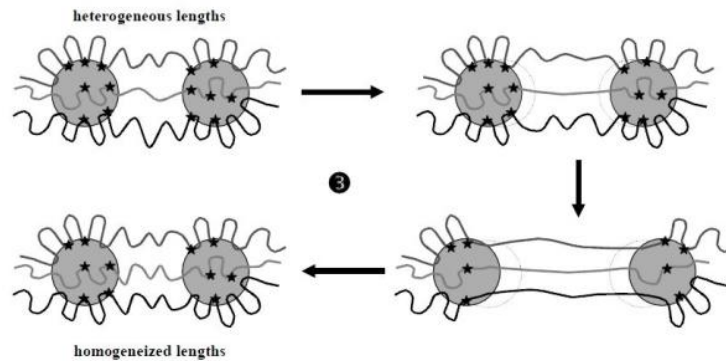


figure 1.16: schematic Dannerberg's model based on molecular slippage mechanism (Mark, Erman, & Eirich, 2005)

Leblac (Leblanc, 2000) proposed another model based on the physical nature of carbon black-rubber interaction. Considering the filler surface topology (as already shown in figure 1.12, section 2.3.1), the overlapping graphitic layers constrain the molecules (figure 1.17): thus a stronger filler-rubber interaction occurs when the surface morphology is perfectly adapted to accommodate the polymeric chains.

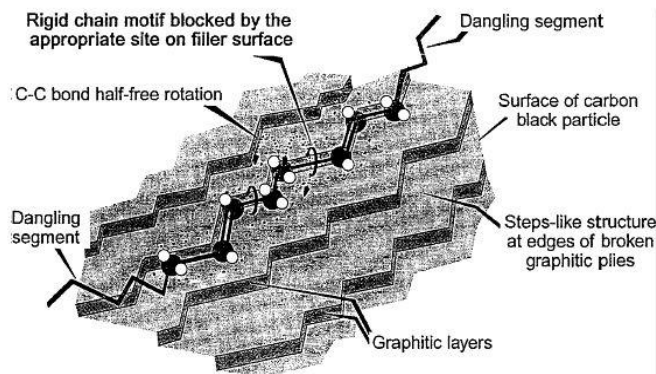


figure 1.17: schematic Leblac's model based on rubber-carbon black physical interaction (Leblanc, 2000)

This part of rubber, directly adsorbed onto the carbon black surface constitutes a layer of macromolecules with lower mobility, generally called "bound rubber". It is a sort of "rubber shell", characterized by a thickness of 0.5-5 nm which cannot be extracted by a good solvent, like toluene, and thus it remains bounded to the filler.

Wolff and Wang studied the interaction of reinforcing fillers with rubber and also with other fillers (Wolff & Wang, 1991). They determined that carbon black aggregates are characterized by a lower ability, than other types of fillers (as silica), to form a filler network in the polymer matrix, but at the same time they interact strongly with hydrocarbon rubber.

In another work, Wolff and Wang deeply studied bound rubber phenomena, considering that filler-rubber interaction is based on the physical adsorption mechanism (Wolff, Wang, & Tan, 1991). They defined that its presence and its amount depend on the properties of filler and of the polymeric matrix: concerning the carbon black its content, its structure, its physicochemical and morphological features are important; as for the rubber the chemical structure of its molecules (saturated or unsaturated, polar or nonpolar) and microstructure (in the sense of configurations and molecular weight, molecular-weight distribution) have to be taken into account. So bound rubber results a complex phenomena considering that it is affected by all these variables. In fact the authors show that the trend of normalized bound rubber for unit area of compounds characterized by different carbon black types but same polymeric matrix and carbon black content decreases as a function of filler surface area (figure 1.18).

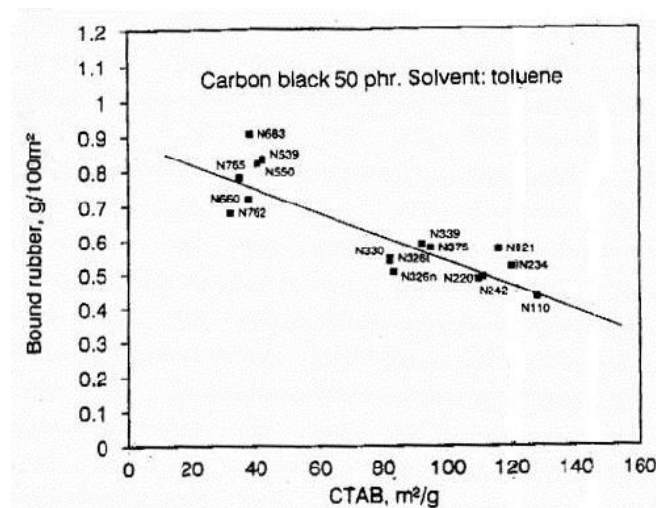


figure 1.18: specific bound rubber as a function of CTAB surface area for different carbon black types at content 50 phr in SBR (Wolff, Wang, & Tan, 1991)

Performing the same kind of analysis considering the effect of carbon black content too, it is possible to observe that the decreasing trend becomes more pronounced for high CB content (figure 1.19). To understand this complex problem some studies were conducted in terms of surface activity (strictly linked to filler surface energy), particles size, carbon black structure and rubber molecular weight.

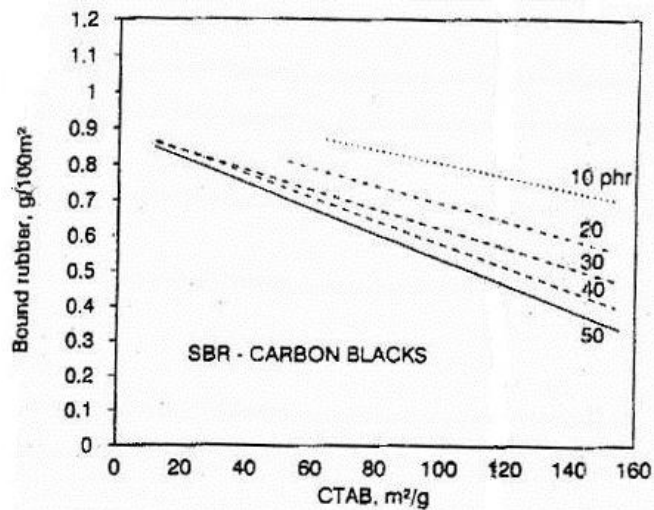


figure 1.19: bound rubber vs. CTAB surface area for SBR filled with carbon black (Wolff, Wang, & Tan, 1991)

2.3.4 EFFECT OF THE FILLER ON MATRIX DEFORMATION

Carbon black fillers are very rigid and curiously, even if they replace part of the volume of deformable phase, they don't reduce the compounds' ability to recover their shape: the increase in modulus does not change much the elongation at break, as it is generally observed for other fillers.

An effect is an amplification of the strain on polymeric matrix with respect to the external deformation (Mark, Erman, & Eirich, 2005).

The hydrodynamic effect is the basis to explain the effect of rigid particles in an elastomeric matrix. Einstein determined an equation for the suspension of spherical rigid particles in an incompressible fluid:

$$\eta = \eta_0 (1 + 2.5 \varphi_f)$$

where η and η_0 are the viscosities of suspension and of the incompressible fluid respectively. This model is not able to take into account the interactions of the particles with other particles or with the surrounding medium.

Guth and Gold generalized Einstein's equation, adapting the viscosity law to predict the small strain modulus of a rubber compound. They added a quadratic term, in order to describe the behavior of filled rubber, where the polymeric chains are adsorbed onto the reinforcing fillers' surface.

$$G^* = G_{rubber}^* (1 + 2.5 \varphi_f + 14.1 \varphi_f^2)$$

In Guth and Gold's equation, the modulus of filled rubbers (G^*) as compared with modulus of the unfilled rubber (G_{rubber}^*) increases with an high content of rigid particles. This relation describes a compound with spherical particles, while filler particles are often not spherical, not well dispersed through the matrix and not fully coated in rubber. Guth derived a modified equation considering a shape coefficient, called average aspect ratio f , defined as the ratio of longest length to its perpendicular width:

$$G^* = G_{rubber}^* (1 + 0.67 f \cdot \varphi_f + 1.62 f^2 \cdot \varphi_f^2)$$

The strain amplification strictly depends on filler content, thus a "strain amplification factor" can be evaluated. Mullins and Tobin derived a relationship (based on Guth and Gold equation) that correlates the macroscopic strain ($\varepsilon = \varepsilon_{compound}$) to the average strain state in the elastomers matrix material (ε_{rubber}), as shown in the following equation

$$\varepsilon_{rubber} = \varepsilon (1 + 2.5 \varphi_f + 14.1 \varphi_f^2)$$

where φ_f is filler volume fraction.

A simple expression for the strain amplification was derived by Bueche in terms of the extension ratio (λ is the extension ratio of filled rubber, while λ_0 is the macroscopic extension ratio)

$$\lambda_{rubber} = \frac{\lambda_0 - \varphi_f}{1 - \varphi_f}$$

Or in terms of strain: the equation assume this form $\varepsilon_{rubber} = \frac{\varepsilon_0}{1-\phi_f}$

2.3.5 EFFECT OF FILLER ON OVERALL COMPOUND PROPERTIES

The properties of rubber compound are strictly influenced by the amount, the size, the surface area, the structure and the chemistry of the filler, so these parameters are chosen considering the final performance of the product. The main field of application is the tire industry, where requirements as rolling resistance, grip and wear resistance are necessary, considering that a tire is subjected to a complex set of forces.

Literature suggests that increasing carbon black aggregate dimension or increasing its structure the crack growth and fatigue resistance of rubber compound improve. On the other side, the choice of carbon black, characterized by small particles increases the abrasion resistance and the tear strength.

Hess and Klamp study the effect of carbon black varying the content and the type (they analyzed 16 different types with different oil content) (Mark, Erman, & Eirich, 2005). The main important results are reached studying the effect on tire rolling resistance. This property appears directly proportional to filler content, but inversely proportional to particles dimensions. In the graph (figure 1.20) the general trend of some other important physical properties as a function of carbon black content are shown.

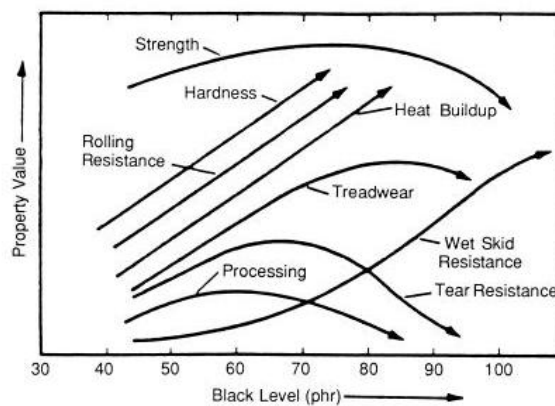


figure 1.20: effect of carbon black content on compound property (Mark, Erman, & Eirich, 2005)

2.4 Stabilizer system and other ingredients

The stabilizer system and other ingredients used for the compound will be briefly described (Mark, Erman, & Eirich, 2005) (Hamed, Materials and Compounds, 2001).

STABILIZER SYSTEM

The stabilizer system is made of antioxidants, antiozonants, that improve the resistance of elastomers from the oxygen and ozone attack. They are necessary because the carbon-carbon double bonds of polymeric chains are very reactive in the presence of these elements, causing chain scission and/or crosslinking. In the first case, the main consequence is softening and decreasing of abrasion resistance, in the case of crosslinking the response of the compound is an increase in hardness and stiffness and reducing fatigue resistance.

It is important to underline that the degradation of rubber is a complex phenomenon, it depends on a large number of factors that interact each other. In addition to oxygen and ozone also thermal heating, light, mechanical stress, the presence of heavy metal contamination, sulfur, oil, solvents can be very dangerous.

OTHER INGREDIENTS

Further ingredients may be added such as pigments, oils, resins, processing aids to improve performance.

The oils are used to improve the processability, but they require specific formulation to be compatible with the polymer and to avoid loss in physical properties. It is usually added after carbon black is well dispersed, because to break the agglomerate/aggregate sufficient shear stresses are necessary, so rubber viscosity must not be too low. The resins improve the dispersion of fillers and wetting of the filler surface, at the same time they decrease the compound viscosity.

3. FRACTURE IN RUBBER COMPOUNDS

In rubber compounds a particular fracture phenomenology is often observed. If a notched sample is loaded in mode I (crack advancement perpendicular to loading

direction), the crack may propagate in two different ways: sometimes it just proceeds along the notch plane but in other cases just one or two cracks propagate in a direction parallel to the loading direction and then a crack propagates along the notch plane. The former cracks are called “sideways” cracks, the latter “forward” crack.

figure 1.21 shows a series of video frames taken during a fracture test, in which sideways cracks developed. They propagate in a steady way and in opposite direction, usually symmetrically.

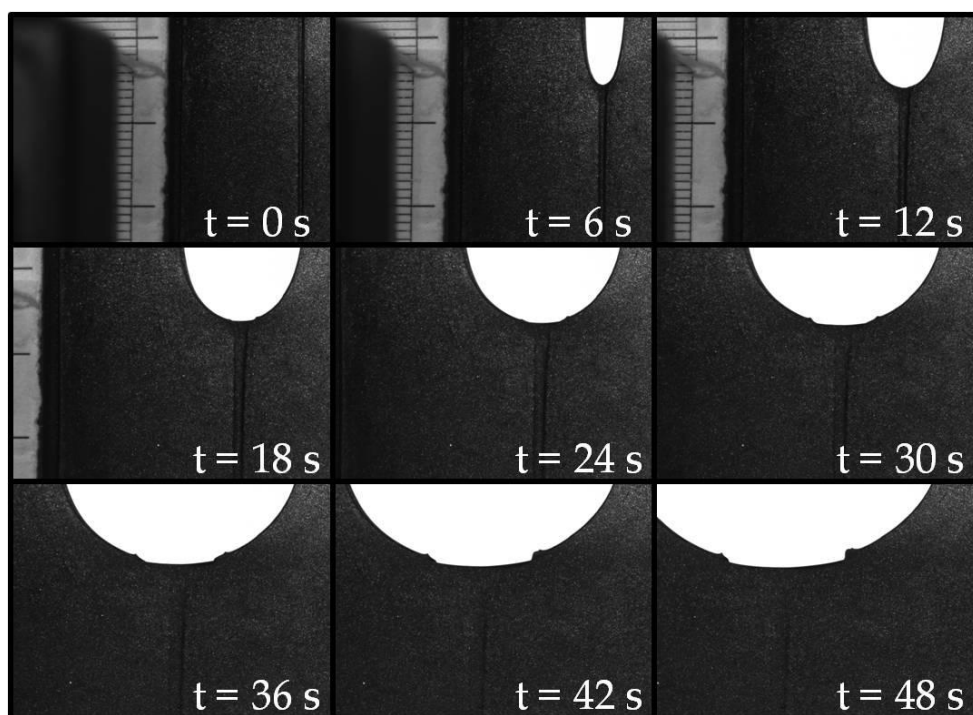


figure 1.21: example of video recorded images sequence test of NRBR/S1.5/CB550-35 at displacement rate 50 mm/min.

*At t = 0 s undeformed state, increasing strain
at t = 6 s sideways cracks initiation,
from t = 6 - 48 s sideways cracks propagation,
at t = 48 s forward crack onset and propagation.*

Sideways cracks initiation has a positive effect on the compounds' toughness: the main effect is to delay the fracture, increasing the toughness of the material. Their formation changes the geometry of the crack tip: increasing its radius, thus reducing stress concentration and enhancing crack growth resistance.

Research works have been performed in order to explain this phenomenology. The deviation of the crack from the expected path is supposed to arise as a consequence of the anisotropy derived from the strained polymeric chains. figure 1.22 schematically illustrates this phenomenology.

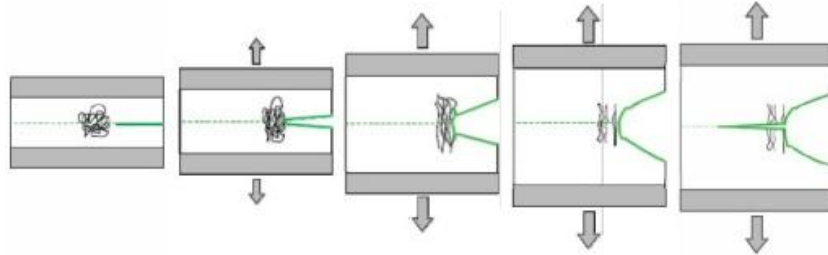


figure 1.22: qualitative physical model of the crack tip during fracture test (Boggio, 2010)

When a notched specimen is strained, the radius of the crack tip increases and the molecular chains, which are in a random coil conformation in the unstrained state, tend to orient preferentially in the loading direction. As deformation increases, their orientation increases, thus the material becomes anisotropic: crack propagation resistance along the notch plane (perpendicular to molecular orientation direction) becomes higher than that in the direction perpendicular to the notch. In this way, the onset and development of sideways cracks in the same direction of applied load is promoted. The condition for sideways cracks onset is determined by the strength anisotropy of the rubber compounds, which is related to the molecular chains orientation (Marano, Boggio, Cazzoni, & Rink, Accepted for publication in press).

In literature (Gent, Razzaghi-Kashani, & Hamed, 2003) based on finite element simulation, it is shown that the energy release rate necessary to initiate a crack parallel to the loading direction is a fraction (0.4-0.6) of the necessary for fracture initiation along the initial notch. The strength anisotropy is linked to the capability of a rubber compound to orient and this is related to the type of rubber, to its crosslink density and to the type and amount of filler (Marano, Boggio, Cazzoni, & Rink, Accepted for publication in press).

As mentioned above once sideways cracks develop, the resistance to forward crack propagation increases due to crack tip blunting and to reinforcing and energy

dissipating mechanism which can occur under large deformation. These phenomena are linked to strain-induced crystallization in the case of stereoregular rubbers, to the breakage and recoiling of chains that have reached their maximum extension (Hamed, 1990) (Hamed, 1994), to re-attachment of broken chains onto fillers particles, to alignment of filler particles in the loading direction.

In conclusion, the toughness of a rubber compound results higher when the phenomenology with sideways cracks is present. This phenomenology is strongly dependent on all components of a compound but their effect is still not completely understood.

2. Materials and methods

1. MATERIALS

The materials adopted in this thesis work are vulcanized rubbers compounds kindly supplied by Bridgestone TCE Srl. .

Three rubber matrices were studied: natural rubber (NR), polybutadiene (BR) and 50/50 blend of them (NRBR).

For each type of matrix, two different series of compounds were considered (table 2.1):

- Same type and amount of carbon black (N550, CB=35 phr), but different sulphur content (S=0.9, 1.5, 2.1 phr);
- Same amount of sulfur (S=1.5 phr) and CB type (N134) but different loading of CB (0, 35, 50, 70 phr).

		CB N 134		
		S = 1.5 phr		
CB [phr]	0	NR/S1.5/CB134-0	BR/S1.5/CB134-0	NRBR/S1.5/CB134-0
	35	NR/S1.5/CB134-35	BR/S1.5/CB134-35	NRBR/S1.5/CB134-35
	50	NR/S1.5/CB134-50	BR/S1.5/CB134-50	NRBR/S1.5/CB134-50
	70	NR/S1.5/CB134-70	BR/S1.5/CB134-70	NRBR/S1.5/CB134-70
		CB N 550		
		CB = 35 phr		
S [phr]	0.9	NR/S0.9/CB550-35	BR/S0.9/CB550-35	NRBR/S0.9/CB550-35
	1.5	NR/S1.5/CB550-35	BR/S1.5/CB550-35	NRBR/S1.5/CB550-35
	2.1	NR/S2.1/CB550-35	BR/S2.1/CB550-35	NRBR/S2.1/CB550-35

table 2.1: studied compounds

These two series of compounds allow to analyze the effect of the different type of carbon black too, due to the available materials having the same sulphur and carbon black content, but different type of CB.

It has to be noticed that the recipes of all compounds are complex, because they contain not only the polymer, vulcanizing agent and fillers, but also other additives in low quantities (see chapter 1 - section 2). One is oil, that is used to facilitate the mixing of the ingredients and the breakage of carbon black agglomerates. Its quantity strictly depends only on the amount of CB: in fact increasing carbon black content, the necessary oil amount increases.

Definition of carbon black (Mark, Erman, & Eirich, 2005)

Two types of CB were considered and their most important properties are reported in table 2.2. As explained in the chapter 1 - section 2.3, the carbon black fillers work as a reinforcement and the different types available can determine different behavior of the compounds. The most influencing factors are the primary particles' dimension, specific surface area and the structure of aggregates.

The type of carbon black is identified by a letter followed by a number. The letter indicates the effect of reinforcing filler on the cure rate of the rubber compound: N stands for normal curing rate, other letters imply that carbon black has been modified to change the curing rate of vulcanization process.

The surface area of the aggregate (NSA) defines the extension of interface, which influences the interaction between elastomers and filler. It is measured through a nitrogen adsorption test. The denomination N134 and N550 refer to fillers having a surface area equal to 143 m²/g and 40 m²/g respectively.

The index, DBP, which indicates the volume of dibutylphthalate absorbed by a given amount of carbon black allows to define qualitatively the shape, giving an indication on how the aggregate structure deviates from the spherical shape. The kinds of carbon black used are characterized by 127 for N134 and 121 for N550. These values are comparable, so it is possible to consider that these aggregates have a similar shape before the compounding.

The index *compressed DBP* has the same meaning of DBP, but in this case the samples are subjected to a series of compressions (4 times to 24000 lb = 10886 kg) before the test. So it gives an indication regarding the change in shape that the filler will undergo during compound processing or in other words how the aggregates break.

	particle size	NSA	DBP	compressed DBP
	nm	m ² /g	-	-
N134	11-19	143	127	103
N550	40-48	40	121	85

table 2.2: properties of carbons black N134 and N550

2. SPECIMEN PREPARATION

All specimens were prepared by compression molding at 160 °C under a pressure of 8 MPa for 15 - 20 - 25 minutes depending on the rubber compound. These conditions were recommended by the Bridgestone TCE Srl. to obtain the proper curing.

The types of samples, which are produced to performed different tests, are obtained using different molds.

3. TEST METHODS

3.1 Crosslink density determination

As mentioned before, the main feature of rubbers is the presence of a network, defined by the crosslinks which tie the macromolecules. In this way, a solvent (like toluene) is not able to dissolve polymeric chains to form an homogeneous solution, but it is absorbed in the network and the rubber swells: to determine the average molecular weight of the chain segments between two junctions, swelling tests are performed. It is important to consider that the junctions are due not only to chemical links, but also to physical bonds, between filler and rubber.

From swelling analysis, it is possible to determine the degree of crosslinking and also the number of monomeric units between two junctions for pure compounds (natural rubber and polybutadiene) because the molecular weight of the single monomeric unit is known.

The specimens did not require a particular geometry. They were cut from molded sheets of each compound, then immersed in toluene. Periodically the weight of swollen rubber was measured until a constant weight was reached, that corresponds to the condition in which the rubber is not able to absorb further solvent. Tests were performed at $23 \pm 2^\circ\text{C}$ and lasted 10 or more days.

The determination of the molecular weight of the segment chains between two junctions is given by Flory- Erman equation (Bokobza, 2004)

$$M_c = \frac{\rho_{\text{compound}} \cdot \left(1 - \frac{2}{f}\right) \cdot V_{\text{molar toluene}} \cdot V_{\text{rubber}}^{1/3}}{\ln(1 - V_{\text{rubber}}) + \chi \cdot V_{\text{rubber}}^2 + V_{\text{rubber}}}$$

Where

ρ is the compound density,

χ is the interaction parameter for the solvent-polymer system ($\chi_{\text{toluene-NR}}=0.39$ and $\chi_{\text{toluene-BR}}=0.34$), for the blend a mean χ value was used.

f is the junction functionality (it is considered equal to 4 for a sulphur curing system),

V_{rubber} is the volume fraction of the polymer in equilibrium condition ($V_{\text{dry network}}/V_{\text{network+solvent}}$)

$$V_{\text{rubber}} = \frac{1}{Q_{\text{rubber}}}$$

$$Q_{\text{rubber}} = \frac{Q_{\text{compound}} - \varphi_{CB}}{1 - \varphi_{CB}}$$

With φ_{CB} that is the volume fraction of the filler (thus considering the studied compounds of carbon black) is defined as

$$\varphi_{CB} = \frac{\frac{m_{CB}}{\rho_{CB}}}{\frac{m_{initial,compound}}{\rho_{compound}}}$$

The degree of swelling of the system is

$$Q_{compound} = \frac{\frac{m_{toluene}}{\rho_{toluene}} + \frac{m_{initial,compound}}{\rho_{compound}}}{\frac{m_{initial,compound}}{\rho_{compound}}}$$

From the molecular weight between two crosslink points it is possible to obtain the degree of crosslinking and the number of monomeric units (N).

$$degree\ of\ crosslinking = \frac{\rho_{compound}}{M_c}$$

$$N = \frac{M_c}{mw_{monomeric\ unit}}$$

3.2 Uniaxial tensile tests

Uniaxial tensile tests were performed adopting dumbbell specimens on all the rubber compounds.

Dumbbell specimens, shown in figure 2.1, were die-cut from 2 mm thick compression molded sheets.

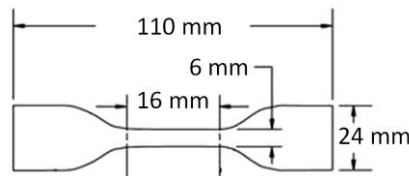


figure 2.1: dumbbell specimen geometry

The experiments were performed at displacement rate of 50 mm/min, using a single column electromechanic dynamometer (Housfield). Displacements along the gauge length were measured by the use of a mechanical extensometer.

The nominal stress was calculated as

$$\sigma = \frac{\text{load}}{\text{cross section}}$$

The strain is the ratio between the displacement measured by extensometer and the initial gauge length:

$$\varepsilon = \frac{\text{knives displacement}}{\text{initial gauge length}}$$

Ultimate stress and strain were determined during the tests.

Stress-strain data were plot using Mooney-Rivlin equation. As deeply treated in chapter 1 - section 1.3, the strain at minimum of the reduced stress curve (σ^* as a function of the inverse of the extension ratio, $\lambda = \frac{l}{l_0} = \frac{l_0 + \Delta l}{l_0} = 1 + \varepsilon$) corresponds to the deformation at which chain segments are able to reach their maximum extension.

$$\sigma^* = \frac{\sigma}{\left(\lambda - \frac{1}{\lambda^2}\right)}$$

In the analysis, the strain at maximum chain extension was considered as an index for the network segments orientability, giving an idea about their capacity of rearrangement under an applied load.

3.3 Dynamic mechanical tests

Dynamic-mechanical tests were carried out in tension on prismatic samples having a cross section of $10 \times 2 \text{ mm}^2$ and a gauge length of 16 mm. They were cut from the same sheets used to obtain the dumbbell specimens for tensile tests.

Dynamic mechanical tests were performed with an RSA II analyser. The testing method adopted consists of the application of a static tensile step by step strain (increasing from 0.05% up to about 200%); at each step a dynamic strain (with a frequency of 10 Hz and an amplitude of 0.05% of the static deformation) is superimposed.

A typical curve of the obtained storage modulus E' as a function of the applied static strain, is reported in figure 2.2: at small strain E' shows a constant value (E'_0), then it decreases to a minimum value (E'_{\min}) and finally it increases again.

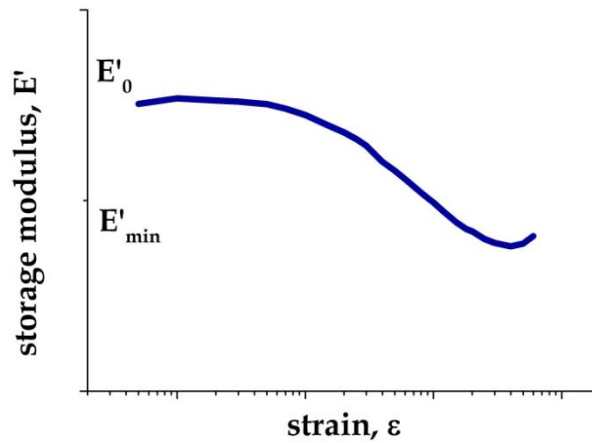


figure 2.2: example of storage modulus-strain curve from dynamic mechanical test and definition of the drop in modulus $\Delta E' = E'_0 - E'_{\min}$ where E'_0 is the constant storage modulus at low strain and E'_{\min} is the minimum at upturn strain

Four contributions of the storage modulus can be distinguished (Fröhlich, Niedermeier, & Luginsland, 2005) (figure 2.3):

- Pure rubber network, due to the chemical crosslinks formed during the vulcanization process with sulfur.
- Hydrodynamic effect, due to the presence of rigid fillers, which are not able to deform, results in a strain amplification effect.
- Filler-rubber interaction, due to physical bonds (Van der Waals) between fillers and polymeric chains (adsorption). This term considers also the layer, characterized by polymeric chains with lower mobility, that surrounds the filler surface.
- Filler network, due to the filler-filler interactions. This network is due to the inter-aggregate interaction, which breaks down as strain increases (Payne effect).

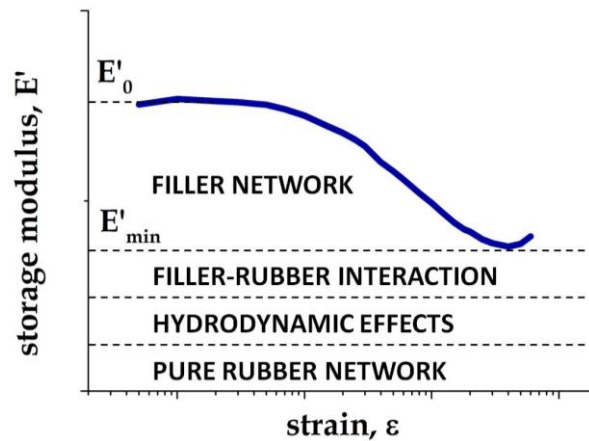


figure 2.3: four contributions of the storage modulus in the storage modulus-strain curve from dynamic mechanical test: pure rubber network, hydrodynamic effects, filler-rubber interaction and filler network

3.4 Fracture tests

Fracture tests were performed in tension adopting the so called pure shear test specimen to determine fracture toughness applying the fracture mechanics approach.

This configuration (figure 2.4) is widely used because, in conditions of constant volume deformations and plane stress ($\sigma_3 = 0$) the pure shear state consists of strain state where no length variation in the direction perpendicular to applied load, so direction 2, occurs ("shear") and no rotations along the principal axes take place ("pure"). In other words, this corresponds to a "constrained tension" (Gent, 2001) because it is a uniaxial tensile test where the deformation in the direction 2 is constrained.

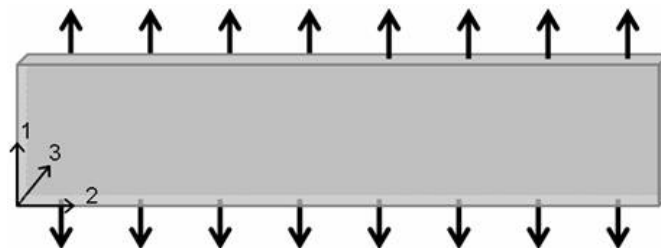


figure 2.4: pure shear specimen

In order to prevent the deformation along the direction 2 and to reduce the lateral contraction (as present in the A region in figure 2.5), a purposely geometry is

necessary: the height of pure shear specimens (direction 1) must be smaller than the width (direction 2), their ratio is normally lower than 1.

For fracture analysis this test specimen with the introduction of a notch was adopted: indeed it was proved that the energy in the region of uniform pure shear is equal to the energy obtained loading un-notched specimen up to its same displacement.

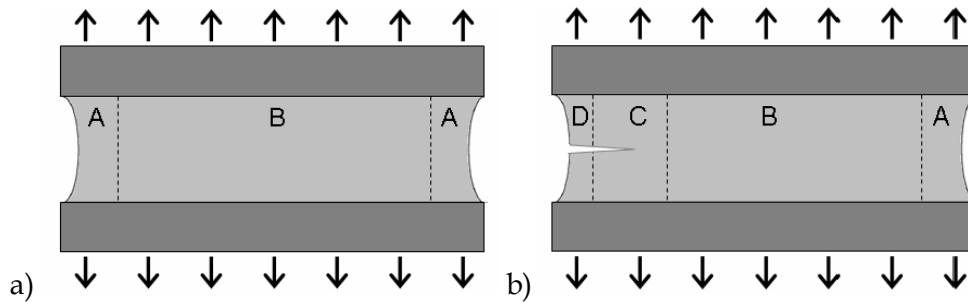


figure 2.5: deformation state in un-notched (a) and notched (b) pure shear specimen

It is interesting that in the notched pure shear specimen four deformation states can distinguish:

- A) State of strain due to the edge effect: the lateral edge is not constrained, so during the deformation it tends to curve inward.
- B) Uniform pure shear state of strain.
- C) Complex state of strain due to notch: an increase of the stress state is present around the notch tip.
- D) Unstrained region.

In this work, two different geometries are adopted: grooved and ungrooved specimens, which type I and type II can be distinguished.

Grooved specimen

To promote crack propagation along the notch plane, a geometry with a groove on both sides of specimen is defined by a purposely-made mold (figure 2.6). The presence of groove makes the cross section lower than the overall specimen thickness. The clamped parts are sustained by reinforced rubber stubs, which are

made of natural rubber with aligned polyamide fibers oriented in the direction of the applied load, used in order to avoid the slippage of the specimen during the test. The notch of 34 mm length was introduced with a cutter and sharpened with a razor blade just before the test.

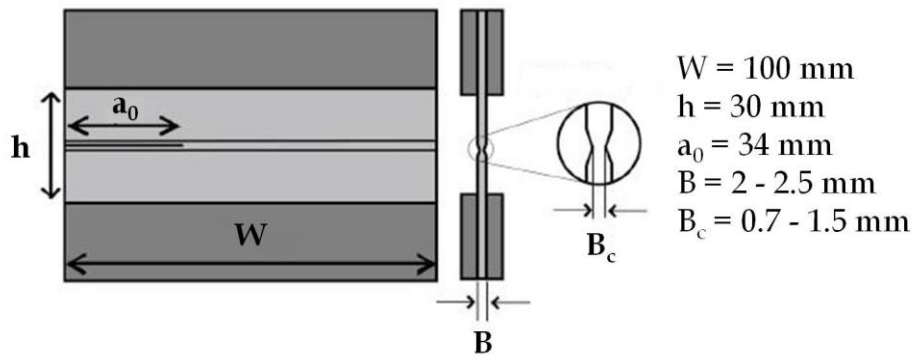


figure 2.6: pure shear groove specimen geometry

Ungrooved specimen: type I

This kind of specimen consists of a rubber sample and reinforced rubber stubs, that are vulcanized together during the vulcanization process. The only difference from the previous geometry is the groove absence (figure 2.7).

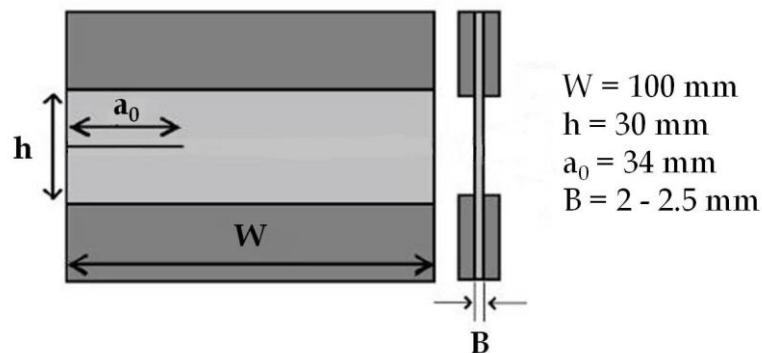


figure 2.7: pure shear ungrooved specimen (type I) geometry

For the preparation of this type of specimens PTFE films are interposed between the compound and the reinforced rubber in the central region, where the vulcanization of the two elements must be avoided. After the crosslinking process, the exceeding part of reinforced rubber is removed (figure 2.8). For fracture test, a notch is created with a cutter and its size measures 34 mm.

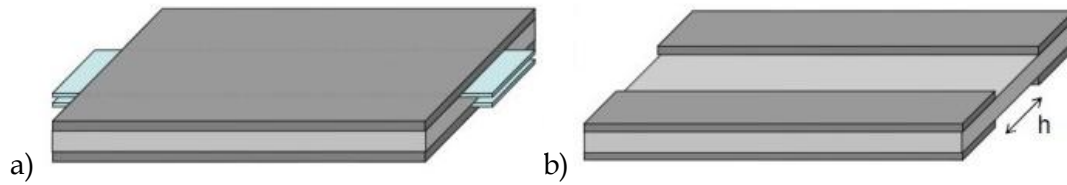


figure 2.8: specimen structure before (a) and after (b) vulcanization process

ungrooved specimen: type II

In a second time a purposely-made mold was used. This specimen has a cross section, as in figure 2.9, which avoids, by using purposely-made clamps, the slippage of the specimen during the test. In this way there is a great saving of materials and time.

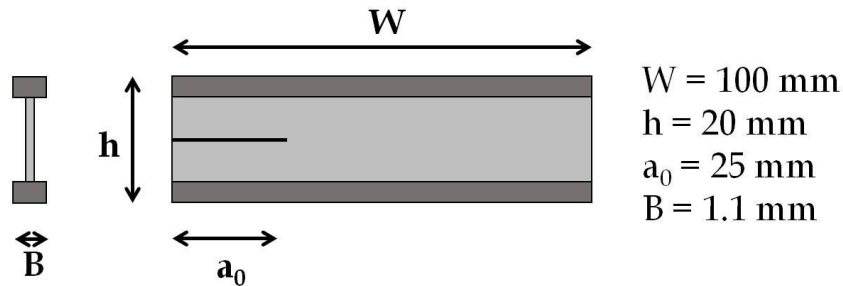


figure 2.9: pure shear ungrooved specimen (type II) geometry

Fracture tests were performed at a displacement rate of 50 mm/min, using an Instron 1185 screw driven dynamometer. Data obtained are crosshead displacement and load as a function of time. Every test was video recorded to observe the fracture phenomenology and to determine the cracks onset.

The value of toughness was evaluated at fracture initiation (cracks onset). The specific moment is individuated with video and then it is defined using load-displacement curve.

J-integral was determine by the expression:

$$J = \eta \frac{U}{B (W - a_0)}$$

where W is the width, a_0 is the initial crack length, $\eta = \eta(a_0/W)$ is a dimensionless factor depending on specimen geometry and on configuration test (which for pure shear configuration is approximately 1 as proved by Hocine (Hocine, Abdelaziz, & Imad, 2002)), the strain energy U is influenced by the displacement, finally B is the sample thickness for ungrooved specimens and the thickness at the notch plane in the grooved specimens ($B = B_c$).

In this work, the dissipated energy was evaluated at the sideways and forward cracks onset, where the strain energy was given by the area under the load-displacement curve in correspondence of the two points, as shown in the image (figure 2.10).

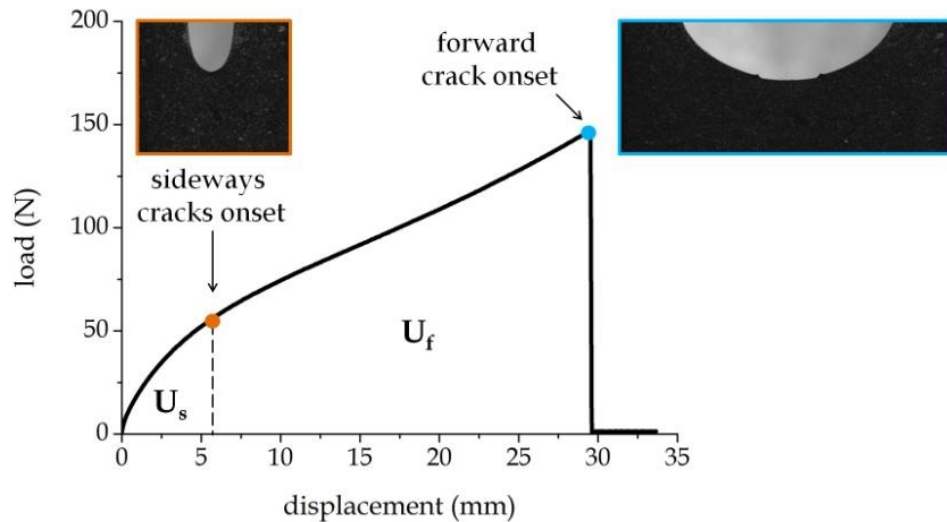


figure 2.10: example of load-displacement curve where the strain energy at sideways and forward cracks onset

LOCAL STRAIN MEASUREMENT

Local strains were also determined on some specimens using Digital Images Correlations (DIC). The software VIC-2D (Correlated Solutions, inc.) was adopted. This technique works comparing images recorded as the material is strained. It appears really interesting and useful for the study of rubbers, because for elastomeric material the use of a contact method, as strain gauges or extensometers, results difficult due to the high level of strain reached (Calabrò, 2013).

It is a valid instrument for a deeper analysis on fracture mode, in fact it allows to determine the local deformation at the crack tip.

The analysis is usually performed on the whole specimen or a portion of it, where the evaluation of strain field is important, for example near the crack tip. This area of interest (AOI) is divided in subsets, that are distinguishable subimages characterized by a square shape (figure 2.11). Its definition is a fundamental part of this analysis, in fact a subset has to contain sufficient information, that make it unique and optically distinguishable from the other subsets. For this purpose, a regular or speckle irregular pattern is applied directly on the specimen surface.

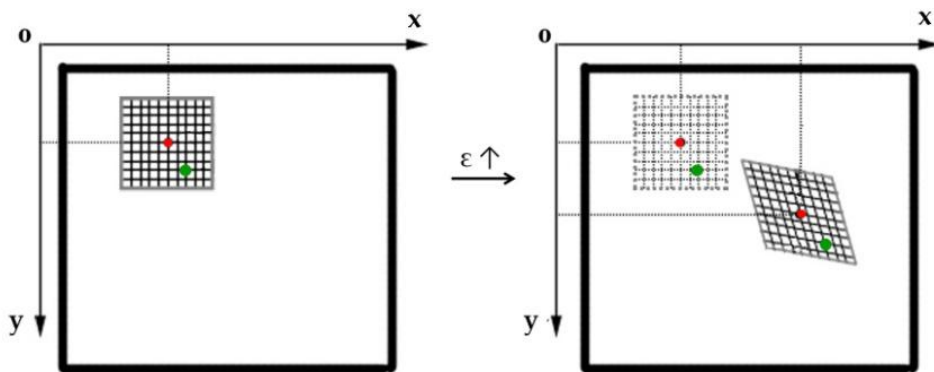


figure 2.11: sketch of subset in the undeformed and deformed image

Another important characteristic to define is the subset step, that individuates the relative spacing between subimages giving a measure of the grid density. Its value is typically less than the size of the subimage. The subsets are characterized by a certain degree of overlap, which depends on how the surface is structured, in fact the non overlapping parts of adjacent subsets have to contain sufficient feature to make them distinguishable. A reliable overlapping is usually in the order of 70-80%.

The field of deformation is obtained through the estimation of speckles displacements, comparing the sequence of images of sample subjected to the applied load to the reference image, which is usually identified with the image in the undeformed state. Treating elastomeric materials, the direct application of this method is difficult: when rubbers reach high level of deformation, the software is not able to correlate the image to the undeformed image. In this case it is necessary

to perform an incremental correlation, that consists of the determination of displacement based on the previous image, so using each image as a reference for the next one.

The measure is influenced by the optical system, depending on the resolution, the image noise, the contrast of the speckle patterns, exposure time, light system and the scale factor, which indicates the number of pixel in 1 millimeter, and by the parameter chosen for DIC analysis (as subset size and subset step).

Another influencing parameter regards the choice of specimen geometry. The images correlation is made difficult due to the presence of the groove along the notch plane, so the measurements of the local strain cannot be performed. In this thesis the speckle pattern was made with a grey paint applied with an airbrush.

3. Results and discussion

As explained briefly in the introduction the purpose of this thesis work is to study the effects of sulfur content, carbon black loading and the type of carbon black on the mechanical behavior of rubber compounds. Sulfur is responsible for chemical crosslinks, generated during the vulcanization process, and thus influences the pure rubber network, CB loading affects the formation of the reinforcing filler network and the final mechanical behavior, and finally the carbon black type may change the interactions of the filler with the elastomeric matrix.

The scheme of the results presentation for each of the three variables considered is made of two parts: the first one regards the effects of the variables on the structure of the compounds (crosslinking density, filler-filler and filler-rubber interactions and the chain extensibility), the second is an attempt to correlate these results with the ultimate mechanical properties of the compound (ultimate stress and strain in tensile tests and fracture toughness from fracture mechanics testing).

1. EFFECT OF SULFUR CONTENT

Natural rubber, polybutadiene and 50-50 blend (NR-BR-NRBR/CB550-35) characterized by three different contents of vulcanizing agent (0.9-1.5-2.1 phr) were analyzed.

1.1 Degree of crosslinking

figure 3.1.a shows the average molecular weight between junctions as a function of sulfur content for NR, BR and the NRBR blend (obtained as reported in chapter 2 section 3.1). M_c decreases as sulfur content increases for the three compounds.

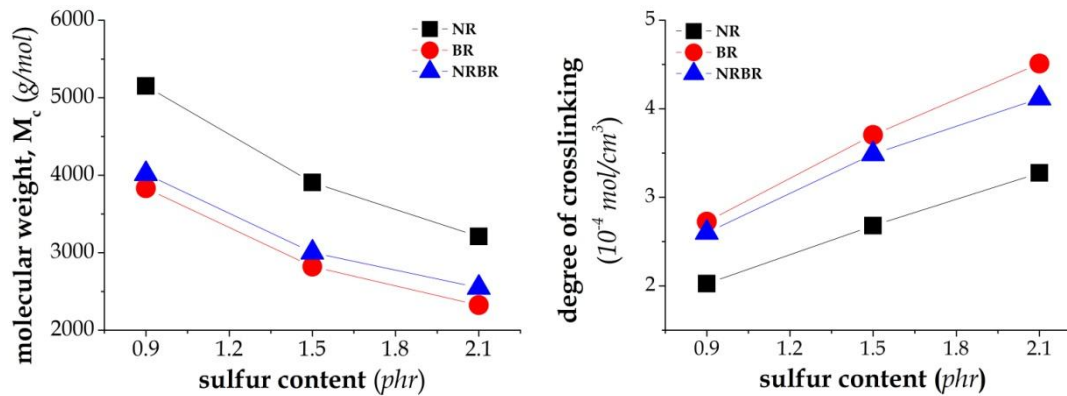


figure 3.1: molecular weight between two junctions (a) and degree of crosslinking (b) for NR-BR-NRBR/CB550-35 as a function of sulfur content

This result is expected since an higher amount of vulcanizing agent produces more chemical junctions, so the chain length between the two crosslink points is reduced. The physical junctions (due to polymer-filler) should be the same, considering that the amount of CB for this series of compounds was always the same (35 phr). The behavior of the blend shows the same trend of the pure compounds but the value of M_c is closer to polybutadiene: in this case physical meaning of M_c value is not so clear.

The molecular weight obtained is the result of both chemical (linked to sulfur) and physical crosslink points (linked to rubber-filler interaction). Comparing the data on the pure compounds with the molecular weight between entanglements ($M_{e,NR} = 7000$ g/mol and $M_{e,BR} = 3000$ g/mol) (Fetters, Lohse, & Colby, 2006) (Chenal, Chazeau, & L., 2007), it is possible to observe that for natural rubber $M_{e,NR}$ is always larger than $M_{c,NR}$, while for polybutadiene $M_{e,BR}$ is similar to $M_{c,BR}$. Therefore it might be expected that, in the case of BR, entanglements may play a role in the compounds' behavior.

The degree of crosslinking is inversely proportional: in fact it is the ratio of the compounds density with the molecular weight of chain segments between two junctions (figure 3.1.b).

1.2 Filler-filler and filler-rubber interactions

From dynamic mechanical analysis the degree of filler-filler and filler-polymeric matrix interactions may be evaluated.

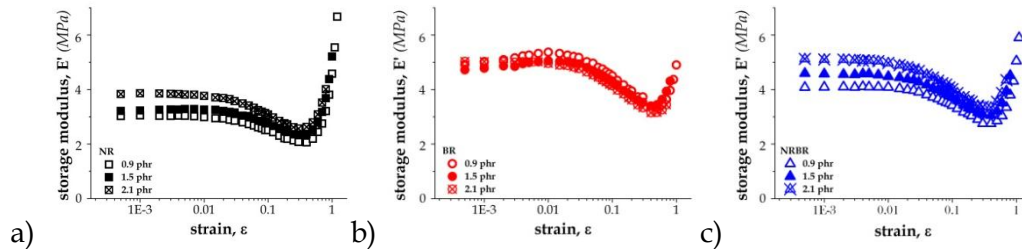


figure 3.2: storage modulus drop E' vs strain for NR(a)-BR(b)-NRBR(c)/CB550-35

figure 3.2 show for the three different rubber matrices, storage modulus E' as a function of strain for the three sulfur contents, all filled with 35 phr CB N550.

Referring to figure chapter 2 – section 3.3, one would expect that E'_{\min} increases as crosslink density increases and that the drop in modulus ($\Delta E' = E'_0 - E'_{\min}$), which reflects the filler-filler interaction, should be constant for each matrix irrespective of sulfur content, since filler type and content are the same.

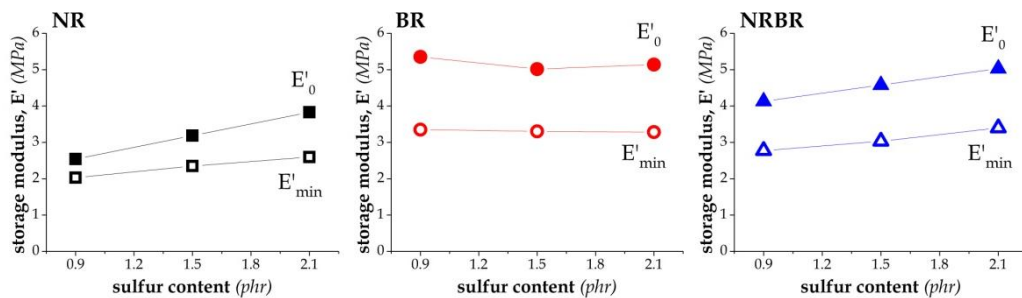


figure 3.3: storage modulus at low strain E'_0 and at the minimum E'_{\min} from DMA of NR(a)-BR(b)-NRBR(c)/CB550-35 as a function of sulfur amount

From figure 3.3, which reports E'_{\min} and E'_0 as a function of S content for the three matrices it is possible to observe that for NR and the blend E'_{\min} increases as S content increases as expected while for BR it remains constant. This could be related to the fact that for natural rubber the molecular weight between entanglements M_e is much longer than the molecular weight between junctions M_c , while for BR M_c and

M_e are comparable. It can also be observed that for BR E'_0 follows the same trend as E'_{\min} thus giving a constant $\Delta E'$, while this is not true for natural rubber for which the drop increases as S content increases (figure 3.4). It seems therefore that for NR also the filler-filler interaction is affected by sulfur content. As for the NRBR blend the behavior seems intermediate.

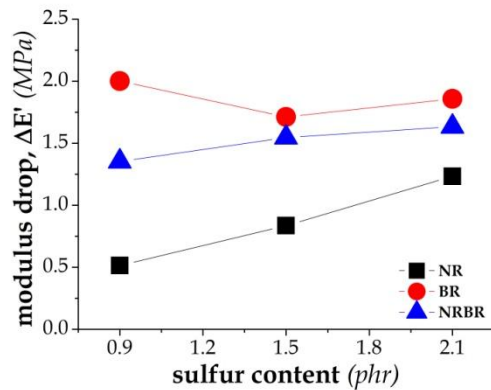


figure 3.4: modulus drop from DMA of NR-BR-NRBR/CB550-35 as a function of sulfur amount

1.3 Strain at the maximum chain extension

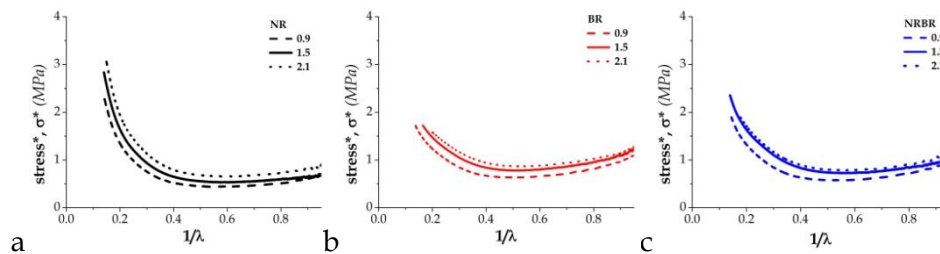


figure 3.5: Mooney-Rivlin plot for NR (a), BR (b) and NRBR (c)/CB550-35

figure 3.5 reports the data obtained in tensile tests following the Mooney-Rivlin equation, i.e. the reduced stress $\sigma^* = \frac{\sigma}{(\lambda - \frac{1}{\lambda^2})}$ as a function of $1/\lambda$, where λ is the extension ratio (see chapter 1- section 1.3). From this plot the strain at the minimum σ^* , considered as the strain for the maximum chain extension, was determined and plotted as a function of sulfur content in figure 3.6.

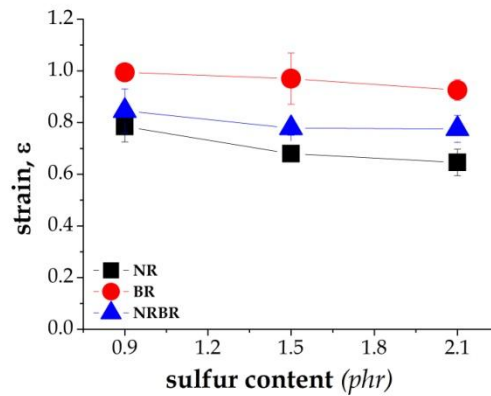


figure 3.6: strain at maximum chain extension for NR-BR-NRBR/CB550-35 as a function of sulfur amount

Using Mooney-Rivlin equation, the deformation at which the chain segments reach their maximum extension was evaluated. It can be observed that the maximum chain extension is lower for natural rubber than for polybutadiene. Further, increasing sulfur content the maximum chain extension for the three matrices is constant or slightly decreasing.

1.4 Ultimate mechanical properties

figure 3.7 reports ultimate stress and strain (σ_R and ϵ_R) obtained in uniaxial tensile test as a function of sulfur content. For natural rubber, stress at break increases with S content while ϵ_R is fairly constant. For BR, instead, σ_R is fairly constant and ϵ_R decreases as sulfur content increases. For the blend ϵ_R slightly decreases while σ_R is constant.

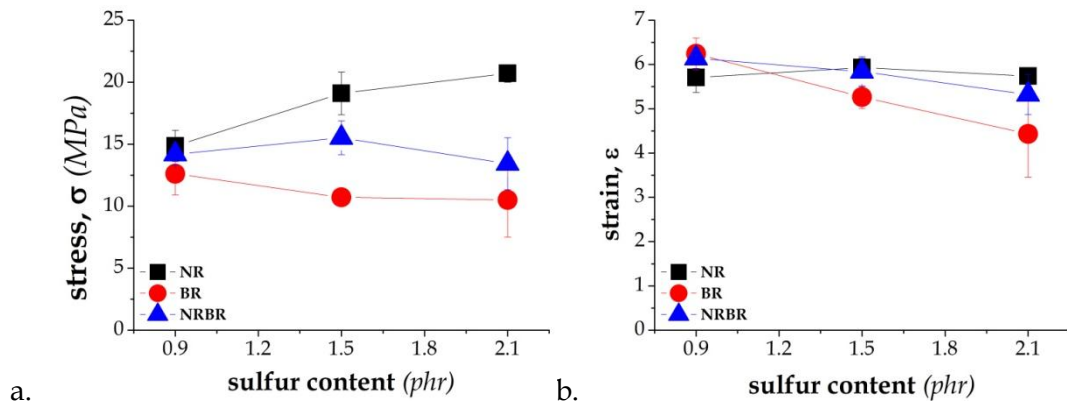


figure 3.7: ultimate stress (a) and strain (b) from uniaxial tensile tests as a function of S content

For fracture behavior two types of phenomenology were observed: crack propagation occurs with or without the formation of sideways cracks (chapter 1 – section 3) depending on matrix type and sulfur content.

Sideways crack formation was not observed in BR compounds irrespective of sulfur content, in NR compounds only for 1.5 and 2.1 phr S, in NRBR compounds it was always arisen. figure 3.8 displays the video frames at forward and sideways (when they were present) cracks onset.

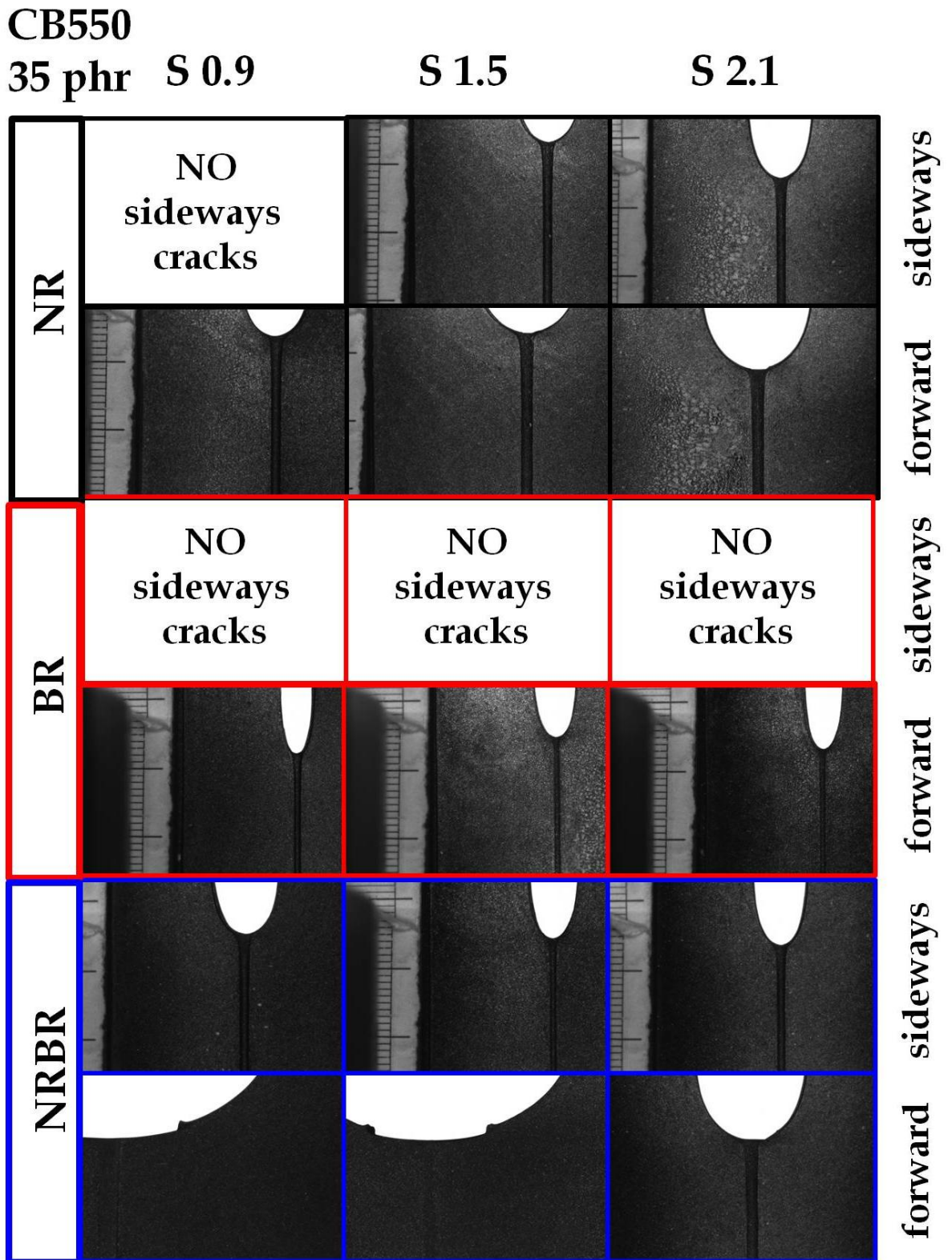


figure 3.8: video frames at sideways and forward cracks onset of NR-BR-NRBR/CB550 as a function of sulfur content

figure 3.9 reports fracture toughness expressed as J-integral at sideways and forward initiation: no particular trend with S content is shown.

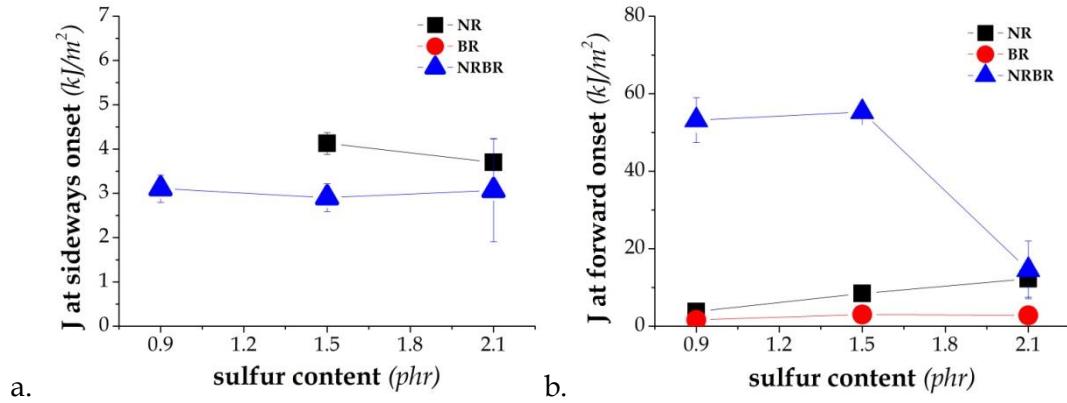


figure 3.9: J at sideways and forward crack onset of NR-BR-NRBR/CB550-35 as a function of sulfur amount using grooved specimen

In polybutadiene compounds, where no sideways crack form, the toughness at forward crack onset is low and fairly constant as sulfur content varies. Its behavior could be related to the fact that M_c for all S contents of BR compounds is close to the critical molecular weight between entanglements and therefore no particular effect of S amount is observed.

As for natural rubber sideways cracks form above a minimum level of sulfur. In this case, since $M_{c,NR} < M_{e,NR}$ the orientability of the molecules depends on S content. The slight decrease in strain at maximum chain extension (figure 3.6) seems to confirm this hypothesis. The toughness at forward crack onset is higher when sideways crack can develop and increases with sulfur content.

The blend appears an interesting material: it shows always the presence of sideways cracks irrespective of sulfur content and on the behavior of the pure compounds at the same S loading.

In particular, NRBR blend with S = 0.9 phr displays sideways cracks even if neither NR nor BR did. Their formation could be explained considering an heterogeneous-two-phase structure of the blend, where the different phases have different stiffness and molecular orientability. NR has lower modulus and great orientability, so for a

given overall strain, the conditions for sideways crack onset could be reached in the NR phase in the blend.

Furthermore, it must be noticed that for $S=0.9$ and 1.5 phr at forward crack onset, the toughness of the blend is almost 10 times larger than that relevant to either of its own parents. When $S=2.1$ phr this is no longer verified J_f relevant to the blend is similar to that of NR.

2. EFFECT OF CARBON BLACK CONTENT

Natural rubber, polybutadiene and 50/50 NR/BR blend with 0-35-50-70 phr of N134 carbon black were studied to determine the carbon black effect on their structure and their ultimate behavior.

2.1 Molecular weight

Performing swelling tests on natural rubber and polybutadiene, the average molecular weight of the chain segments between chemical and physical junctions and the network density were evaluated. As reported in figure 3.10 the increase of carbon black loading determines a decrease of the molecular weight for both the tested compounds.

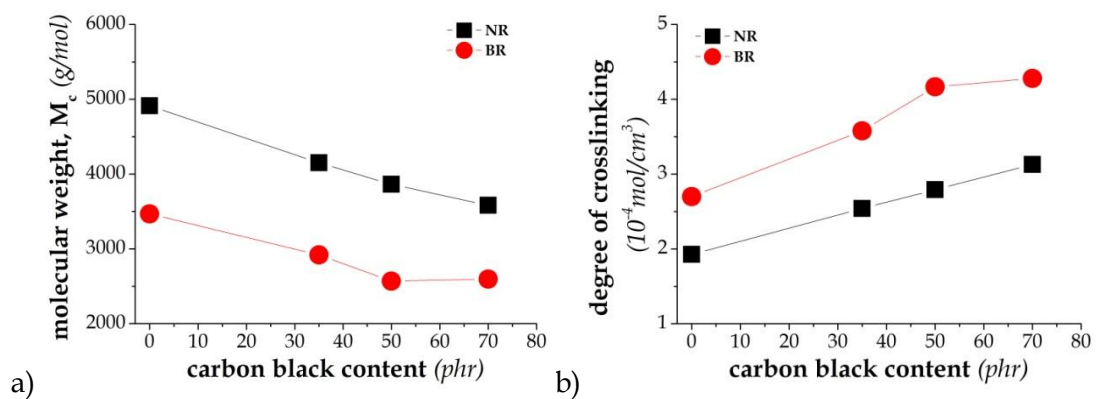


figure 3.10: molecular weight of the chain segments between two junctions (a) and degree of crosslinking (b) of NR-BR-NRBR/S1.5/CB134 as a function of CB content

Comparing these results with the molecular weight between two entanglements (Fetters, Lohse, & Colby, 2006) (Chenal, Chazeau, & L., 2007), the data obtained show that $M_{c,NR}$ of NR compounds are always lower than the reference value $M_{e,NR}$ equal to 7000 g/mol.

The situation is different for BR: the molecular weights between two crosslink points of the all CB contents compounds are comparable with the molecular weights between two entanglements ($M_{c,BR} \approx M_{e,BR} \approx 3000$ g/mol). This means that the entanglements may influence the mechanical behavior irrespective to the degree of crosslinking.

2.2 Filler-filler and filler-rubber interactions

Dynamic mechanical analysis (DMA) was carried out in order to determine the effect of carbon black content on the filler network and on CB interaction with the polymeric matrix.

The figure 3.11 displays the typical curves of the storage modulus as a function of strain for natural rubber, polybutadiene and their blend related to the four CB loadings. It is observed that increasing CB content, the storage modulus increases. In particular, as reported in the chapter 1 - section 3.3, it is expected that increasing the degree of crosslinking due to the higher amount of physical junctions, the hydrodynamic effect, the filler-rubber interactions and the filler network could be affected. The modulus at the minimum E'_{min} and the modulus drop ($\Delta E' = E'_0 - E'_{min}$) should grow.

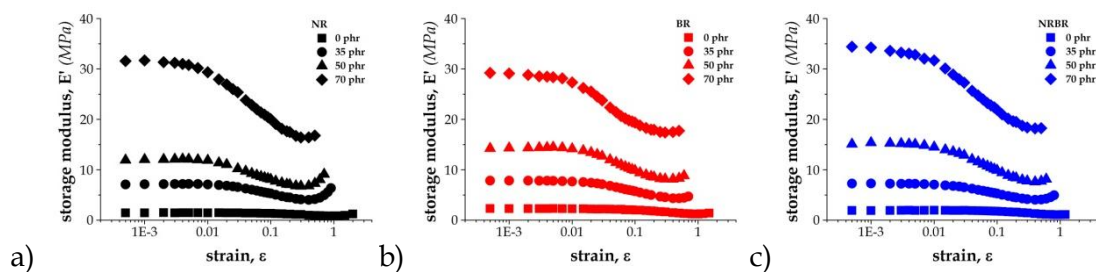


figure 3.11: storage modulus curve from DMA of NR(a)- BR(b)-NRBR(c)/S1.5/CB134 for different CB content as a function of strain

The figure 3.12 shows that E'_{min} increases with CB content: all the rubber compounds have the same trend, thus it seems that the three contributions already mentioned behave in the same way for the different polymeric matrices NR, BR and NRBR.

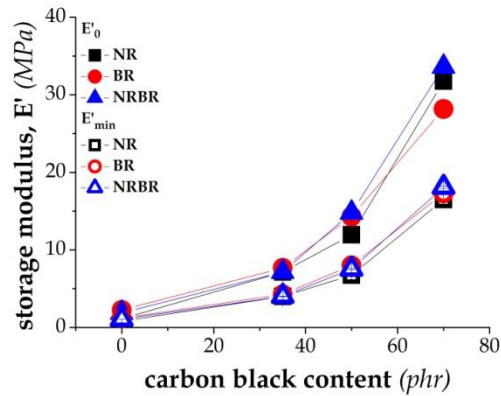


figure 3.12: storage modulus at low strain (E'_0) and at minimum (E'_{min}) of NR-BR-NRBR/S1.5/CB134 as a function of CB content

Applying the Guth-Gold equation, mentioned in the chapter 1 section 2.3, it was tried to evaluate the hydrodynamic effect: it does not contribute significantly to the increase of the modulus.

Therefore the higher E'_{min} with the increase of CB should depend on the pure rubber network and on the filler-rubber interaction. In particular this last contribution is linked to the physical interactions between the polymeric matrix and carbon black (adsorption) and to the “bound rubber”, which consists of a layer of polymeric chains surrounding the aggregate surface with lower mobility (see chapter 1 – section 2.3.3).

The modulus drop ($\Delta E'$) as a function of carbon black loading, which is reported in figure 3.13, increases: it reflects the filler network, therefore the interactions between the layers of bound rubber of the reinforcing fillers. For the three compounds with low CB content, the filler-filler interaction is the same, while for high loading the modulus drop varies as function of polymeric matrix, suggesting different dissipating mechanisms.

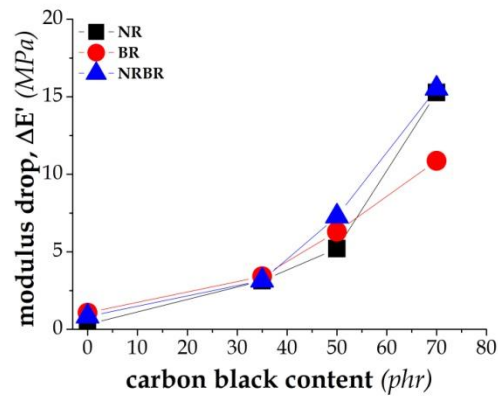


figure 3.13: modulus drop of NR-BR-NRBR/S1.5/CB134 as a function of CB content

Furthermore, in order to investigate the effect of carbon black content on the absolute reinforcement, the modulus had to be analyzed independently to the type of rubber matrix, thus the normalized storage modulus respect the modulus of the matrix or unfilled rubber was calculated. It was plotted as a function of the strain, as reported in figure 3.14. Carbon black loading does not influence the reinforcement, in fact at the same CB content natural rubber always shows higher modulus than polybutadiene and the blend.

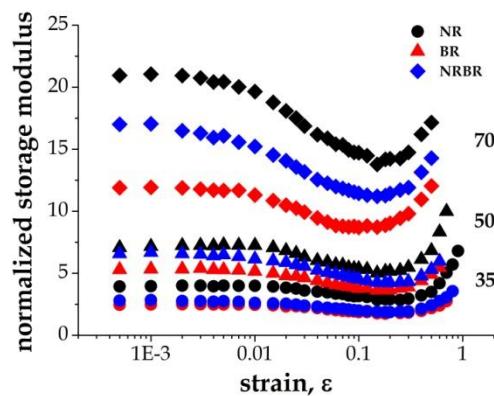


figure 3.14: normalized storage modulus of NR-BR-NRBR/S1.5/CB134 at CB content as a function of strain

2.3 Strain at maximum chain extension

Mooney-Rivlin plot is a useful representation to determine the deformation at which the chain segments reach their maximum extension.

The curves for natural rubber, polybutadiene and their blend with different CB loading are reported in figure 3.15. It is observed that at large strains increasing filler content, the deviation from linearity due to the strain induced crystallization (see chapter 1 section 1.3) is more pronounced. Only unfilled BR seems not able to crystallize.

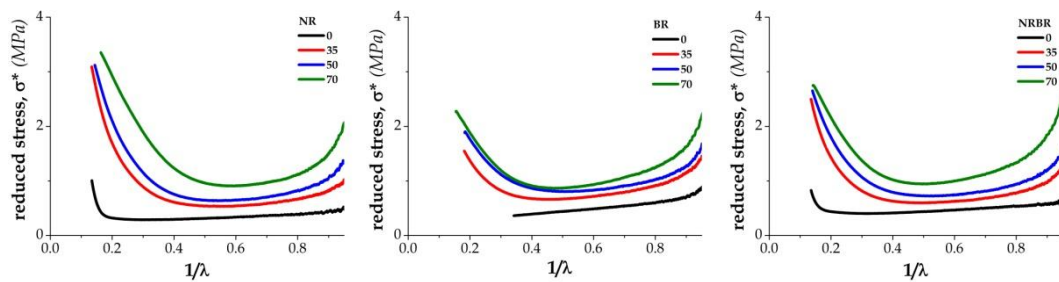


figure 3.15: Mooney-Rivlin plots of NR, BR and NRBR/S1.5/CB134 with different CB content

The figure 3.16 shows the deformation at maximum chain extension as a function of carbon black content. The presence or absence of reinforcing fillers affects significantly this value: for each unfilled compound the strain is high, while for filled rubbers the trend appears constant or slightly decreasing with CB amount.

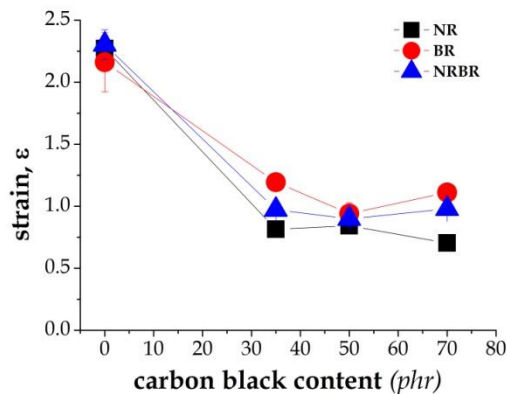


figure 3.16: strain at the maximum chain extension of NR-BR-NRBR/S1.5/CB134 as a function of CB content

2.4 Ultimate mechanical behavior

The ultimate stress and strain obtained performing uniaxial tensile tests are reported in the figure 3.17.

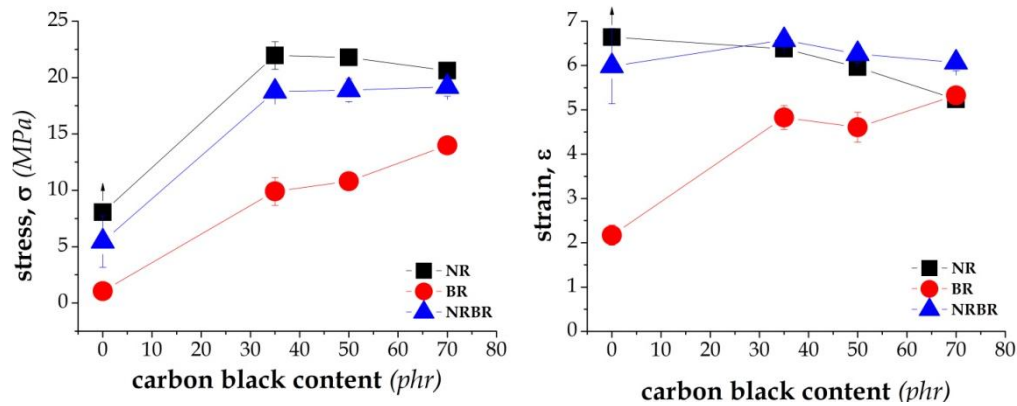


figure 3.17: ultimate stress and strain of NR-BR-NRBR/S1.5/CB134 as a function of carbon black content, unfilled NR did not break up to the maximum possible experimental strain.

Focusing on σ_R , the presence of reinforcing fillers increases the mechanical strength. For the filled compounds increasing carbon black content, for the blend the ultimate stress is constant, for natural rubber it slightly decreases, while for polybutadiene it increases.

As for ϵ_R the trend is more regular as filler increases from 0 phr to 70 phr content, for NR ultimate strain decreases, for BR increases and for NRBR blend it appears constant.

Fracture tests with pure shear ungrooved specimens were performed to evaluate the fracture behavior. Most of the studied compounds show the typical fracture phenomenology (see chapter 1 section 3) as reported in the video frames in figure 3.18. Only unfilled rubbers and BR/S1.5/CB134-35 don't display the formation of sideways cracks. As the reinforcing filler amount increases, the crack tip at the sideways cracks onset appears less deformed, while at forward crack initiation it seems more deformed but the trend is less clear. Comparing the three unfilled compounds, for NR the radius at the crack tip appears more deformed than for BR and the blend.

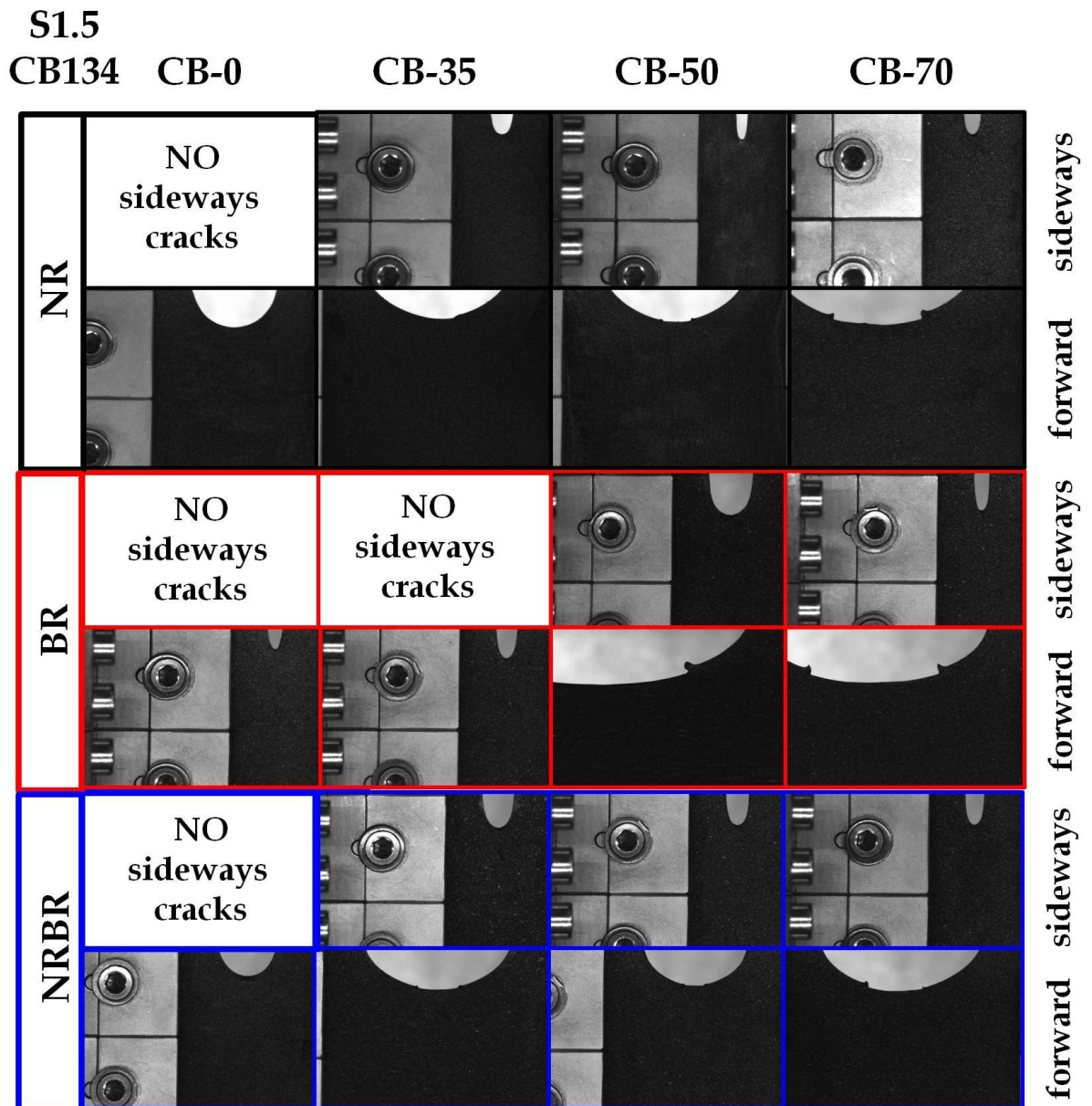


figure 3.18: video frames at sideways and forward cracks onset of NR-BR-NRBR/S1.5/CB134 as a function of carbon black content adopting new specimen geometry

Since ungrooved specimen were adopted, it was possible to perform DIC analysis and the local strains at the crack tip were determined.

In figure 3.19 for each compound the local strain at the crack tip and the deformation at the maximum chains extension are compared. Also the overall strain measured from the crosshead displacement is reported.

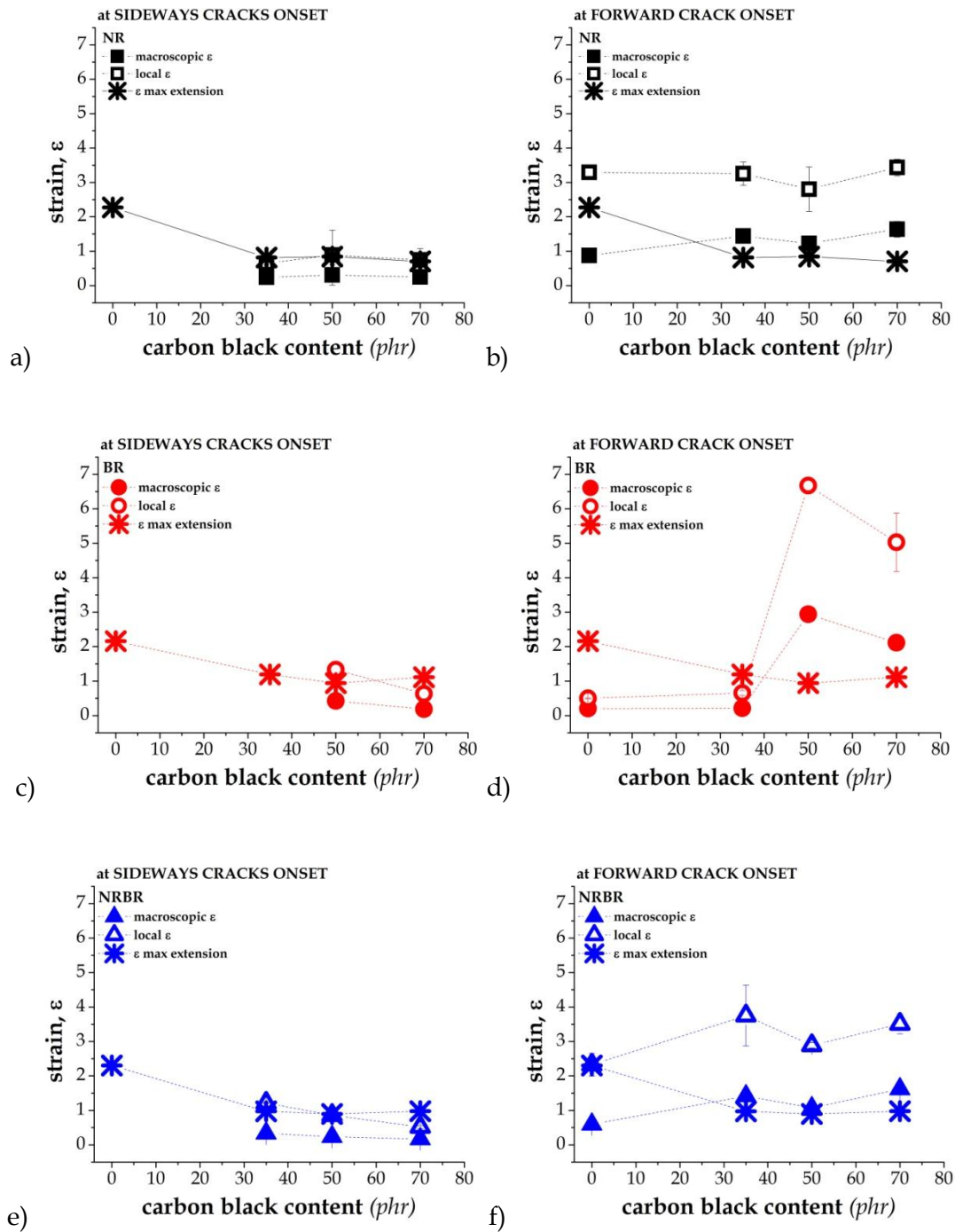


figure 3.19: macroscopic strain, local strain and strain at maximum chain extension at sideways and forward cracks onset of NR (a,b), BR (c,d), NRBR (e,f) S1.5/CB134 as a function of carbon black content

For NR, BR and NRBR it is observed that sideways cracks onset occurs when the local strain at the crack tip is comparable with the deformation at which the network chains reach their maximum extension. For BR/S1.5/CB134-35, which does not

form sideways cracks, fracture occurs before reaching the maximum extension of network chains as shown in figure 3.19.d. In unfilled rubbers where no sideways crack develop the forward crack onset occurs at strains larger than the strains at maximum chain extension.

The J-value, J_s , at the sideways cracks onset as a function of carbon black content (figure 3.20) slightly decreases for the all rubber compounds. It is true even if the data scatter in some cases is consistent.

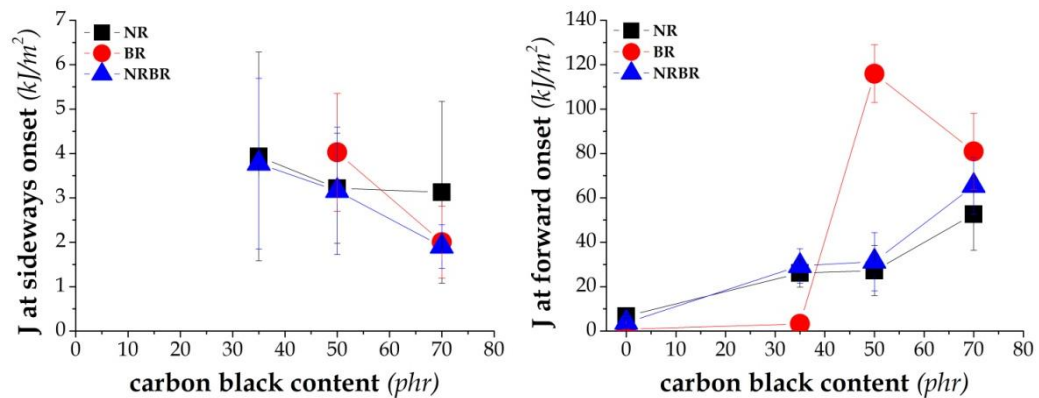


figure 3.20: J at the sideways and forward cracks onset of NR-BR_NRBR/S1.5/CB134 as a function of carbon black content

The fracture toughness at the forward crack onset, J_f , is reported in figure 3.20 as a function of the carbon black content: when no sideways cracks develop low toughness is found (unfilled rubbers and polybutadiene with 35 phr CB).

It is observed that for natural rubber and the blend J_f increases CB content increases: in particular for both compounds with 35 phr and 50 phr J_f values are comparable. Polybutadiene shows low fracture toughness for unfilled and the 35 phr compound, very high value for 50 phr and for 70 phr content it decreases significantly. This means that the higher degree of crosslinking affects negatively this compound.

Fracture toughness for the three rubber compounds were compared with data from a previous work (Cazzoni, Calabrò, Marano, & Rink, 2013), made in Politecnico di Milano, on the same type of rubber compounds supplied by Bridgestone TCE., but from a previous batch. Moreover fracture tests were performed using pure shear

specimens with groove (as shown in chapter 2 – section 3), while in this work pure shear specimens without groove (type II) were adopted.

In figure 3.21, fracture toughness of the two different batches are compared. It can be observed that data from (Cazzoni et al.) show a more regular trend than those obtained in this thesis. In particular natural rubber and the blend with carbon black contents equal to 50 phr and polybutadiene with 70 phr are characterized by a lower fracture toughness than the paper.

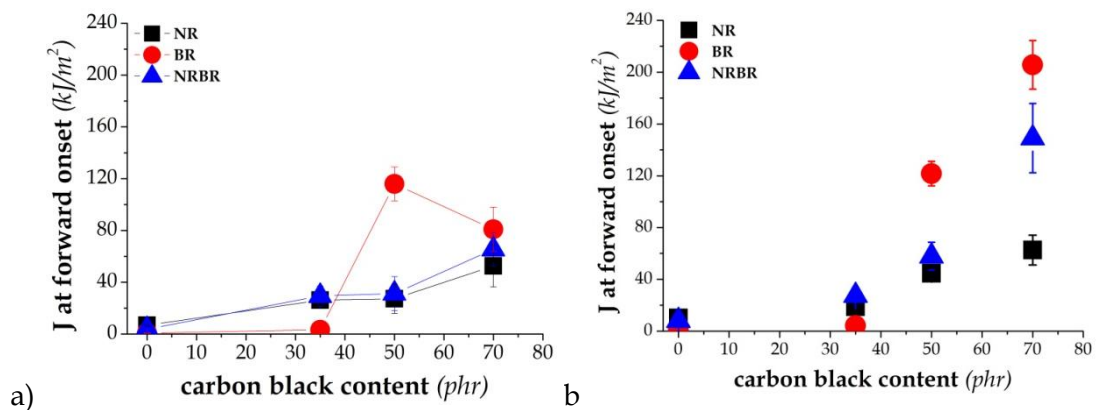


figure 3.21: fracture toughness comparison between thesis results (a) and literature data (b)(Cazzoni, Calabrò, Marano, & Rink, 2013)

This different trends could be due to the different batches or the different test specimen geometries. Both were checked.

Different samples having a different height over width ratio (h/w) and grooved or ungrooved as described in chapter 2 – section 3.3 were tested for NR compound with 35 and 50 phr carbon black. The effect of specimen geometry appears negligible.

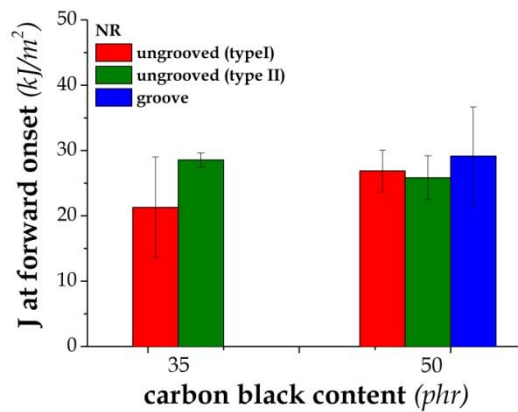


figure 3.22: energy released at forward crack onset of NR/S1.5/CB134-35 and 50 with different combination of batch material and specimen geometry

The stress-strain curves of both batches of rubber compounds for NR with 50 phr of carbon black and polybutadiene filled with CB 70 phr are compared in figure 3.23 : they show slight differences at high strains.

This comparison was carried out also for the other compounds, for which stress-strain curves were perfectly superimposed.

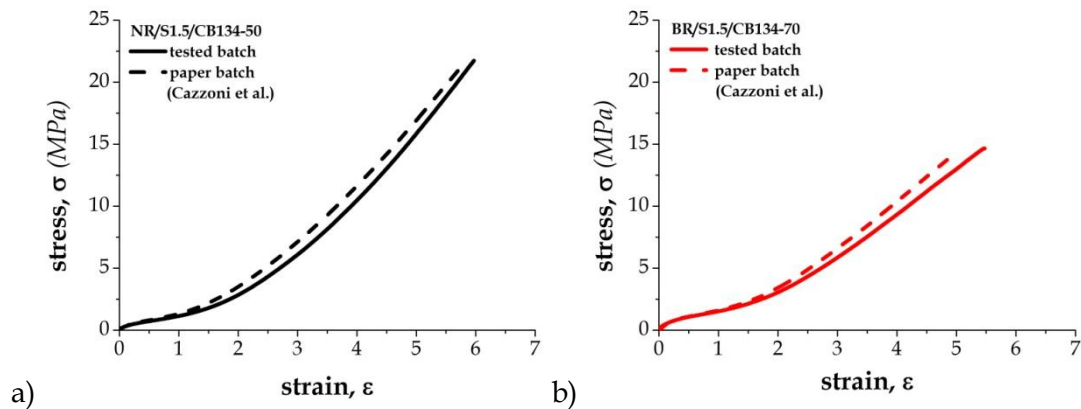


figure 3.23: comparison of stress-strain curves of NR/S1.5/CB134-50 and BR/S1.5/CB134-70 characterized by different batch

Therefore the different behavior observed is probably due to some small difference in the two batches of compounds, indicating that the fracture behavior of polybutadiene with 70 phr of carbon black is strongly dependant on the compound formulation.

3. EFFECT OF CARBON BLACK TYPE

The effect of carbon black type was analyzed considering N134 and N550, having different surface area, but similar structure. They were added to natural rubber, polybutadiene and the blend in the same quantity (35 phr). All these compounds were crosslinked with 1.5 phr of sulfur.

3.1 Degree of crosslinking

The average molecular weight of the network chains between two junctions was evaluated carrying out swelling test in toluene and the result is reported in figure 3.24.a together with that of the relevant crosslinking density (figure 3.24.b). it appears that M_c is slightly increasing as aggregate surface area increases.

The increase is very limited if compared with that determined by a change in sulfur content (figure 3.1.a in chapter 3-section 1.1) or in CB loading (figure 3.10 in chapter 3-section 3.1).

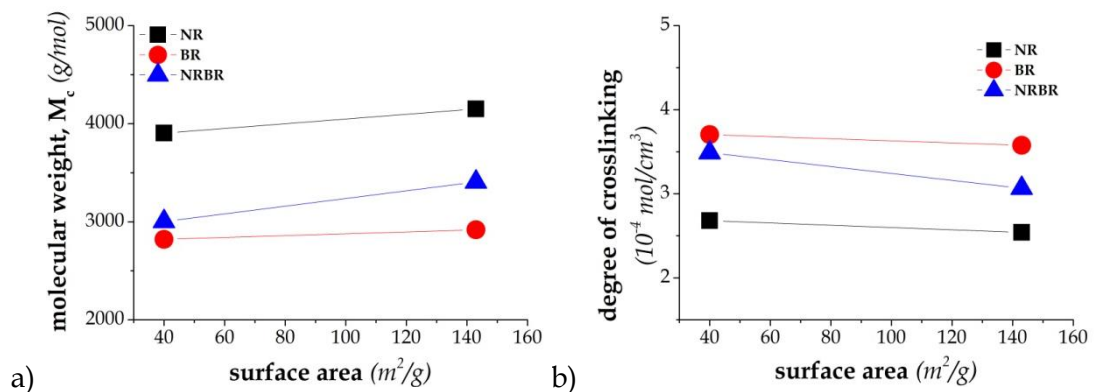


figure 3.24: molecular weight of the chain segments (a) and degree of crosslinking (b) of NR-BR-NRBR/S1.5/CB35 as a function of different carbon black types

3.2 Filler-filler and filler-rubber interactions

The comparison of the storage modulus curve for the three rubber compounds, obtained from DMA, as a function of the applied strain shows that both, the low strain modulus E'_0 and the minimum value of modulus E'_{\min} , are affected by the type of carbon black (figure 3.25).

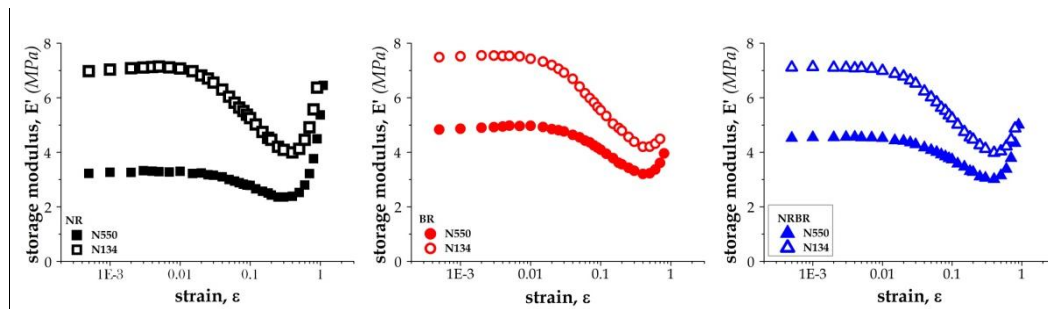


figure 3.25: storage modulus curve from DMA of NR(a)- BR(b)-NRBR(c)/S1.5/CB35 as a function of strain

In (Fröhlich, Niedermeier, & Luginsland, 2005) it was found that as the surface area increases E'_0 increases while E'_{\min} does not change, indicating a greater extent of the filler network. Further the effect of CB structure at constant surface area was to increase both E'_0 and E'_{\min} maintaining the same difference between the two. The two carbon black types (N550 and N134) have very different surface area but also their structure appears somewhat different specially in terms of CDBP (tab. Chapter 2-section 1).

The figure 3.26.a reports E'_0 and E'_{\min} as a function of surface area. Both contributions increase as surface area increases. Following (Fröhlich, Niedermeier, & Luginsland, 2005) in a first approximation, the increase in E'_{\min} could be related to the different structure of the carbon blacks, while that of E'_0 is due to both, structure and surface area. The difference ($\Delta E' = E'_0 - E'_{\min}$), reported in figure 3.26.b, would show the effect of the increase of surface area.

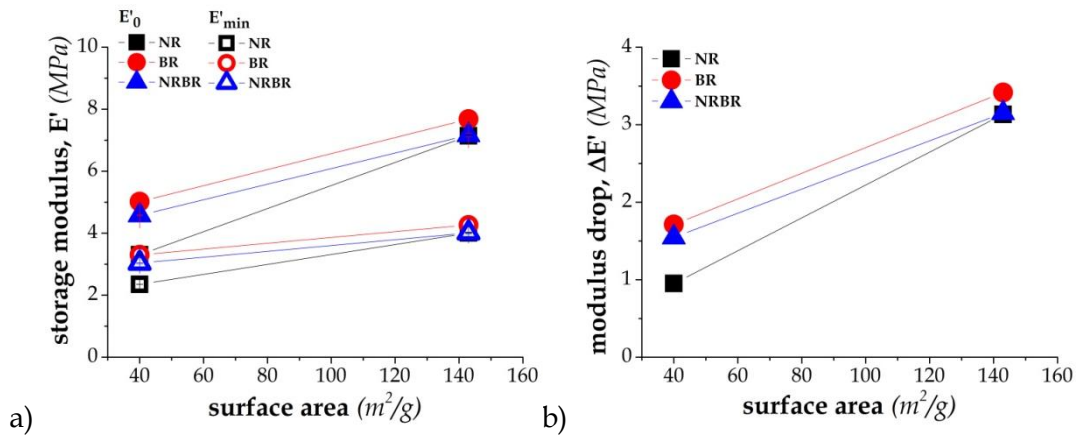


figure 3.26: storage modulus at low strain (E'_0) and at the minimum (E'_{min}) (a) and modulus drop ($\Delta E'$) of NR-BR-NRBR/S1.5/CB35 as a function of different carbon black types

To better compare the three matrices in terms of reinforcement, the storage modulus was normalized as a function of the matrix modulus. In figure 3.27 the DMA curves relevant to the two types of carbon black are reported: NR with CB N134 show the most effective reinforcement. Adopting carbon black with lower surface area (N550), the differences is less appreciable.

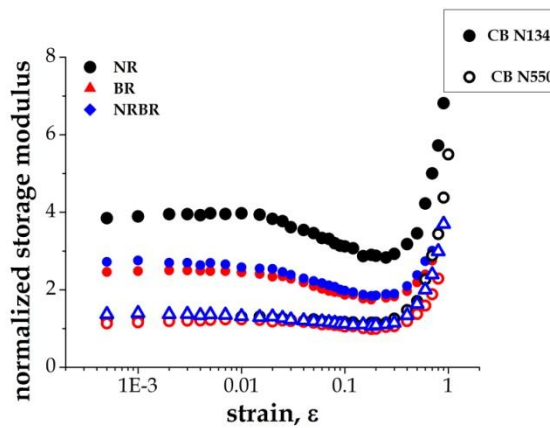


figure 3.27: normalized storage modulus of NR-BR-NRBR/S1.5/CB35 as a function of carbon black surface area

3.3 Strain at the maximum chain extension

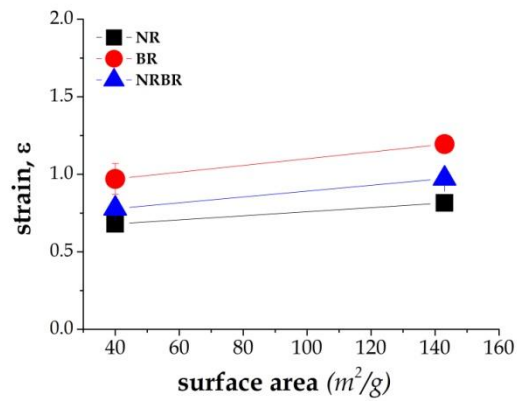


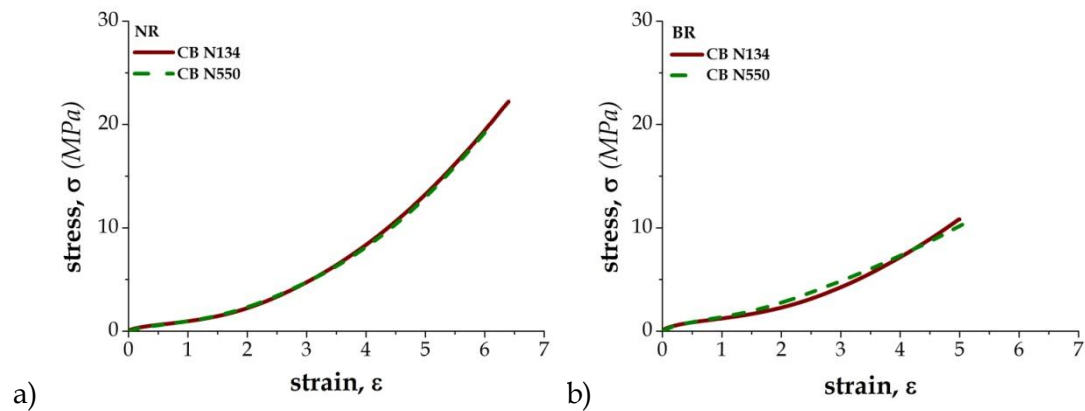
figure 3.28: strain at the maximum chain extension of NR-BR-NRBR/S1.5/CB35 as a function of carbon black surface area

figure 3.28 reports the strain at the maximum chain extension for the three matrices as a function of surface area. Higher value is observed for N134.

The trend is consistent with that of the average molecular weight between two junctions (figure 3.24).

3.4 Ultimate mechanical properties

Stress strain curves obtained from uniaxial tensile tests are reported in figure 3.29.



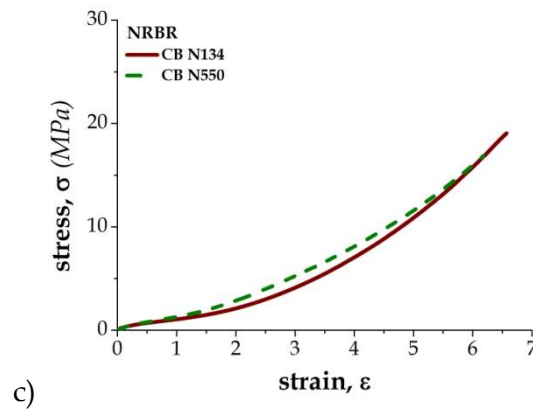


figure 3.29: stress-strain plots from uniaxial tensile tests for NR(a)-BR(b)-NRBR(c) S1.5/CB35 with different CB type

For NR the curves with the different carbon black type are superimposed. While, for polybutadiene and the blend at intermediate values of deformations a slight difference is observed.

The following figure 3.30 shows the ultimate stress and strain for different CB-type rubber compounds: natural rubber and the NRBR blend have the same trends, while polybutadiene behaves in the opposite way. Increasing filler surface area, for polybutadiene σ_R does not change, while for natural rubber and the blend it increases. The ultimate strain is not largely influenced by the CB type, the variation of ϵ_R is not significant.

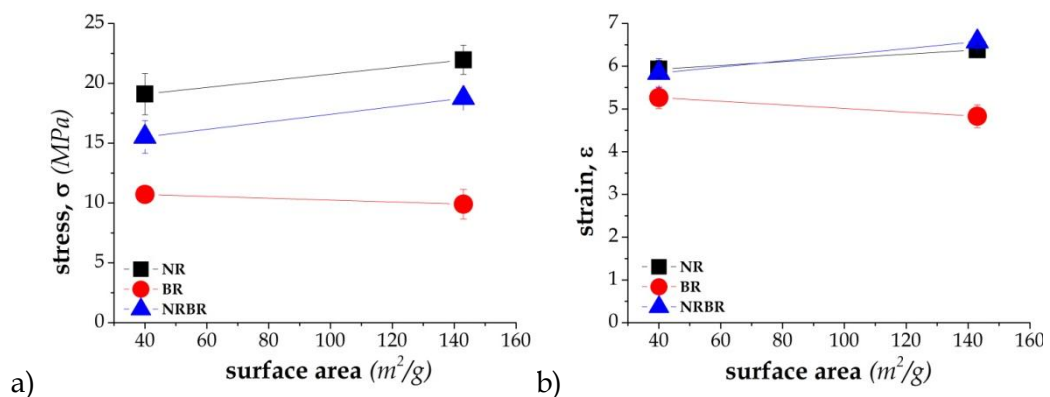


figure 3.30: ultimate stress (a) and ultimate strain (b) of NR-BR-NRBR/S1.5/CB35 as a function of carbon black surface area

Fracture tests were performed on different specimen geometries: compounds with CB-N550 on grooved sample, while compounds with CB-N134 on un-grooved specimen type II. The effect of geometry on the fracture toughness is negligible, as verified in literature (Marano, Boggio, Cazzoni, & Rink, Accepted for publication in press) and also as already proved in the previous section (chapter 3-section 2.4).

In figure 3.31, the video frames at sideways and forward cracks were reported: polybutadiene shows only forward crack initiation irrespective of the filler surface area, while in natural rubber and in the NRBR blend sideways cracks are present, in particular they develop symmetrically in the blend.

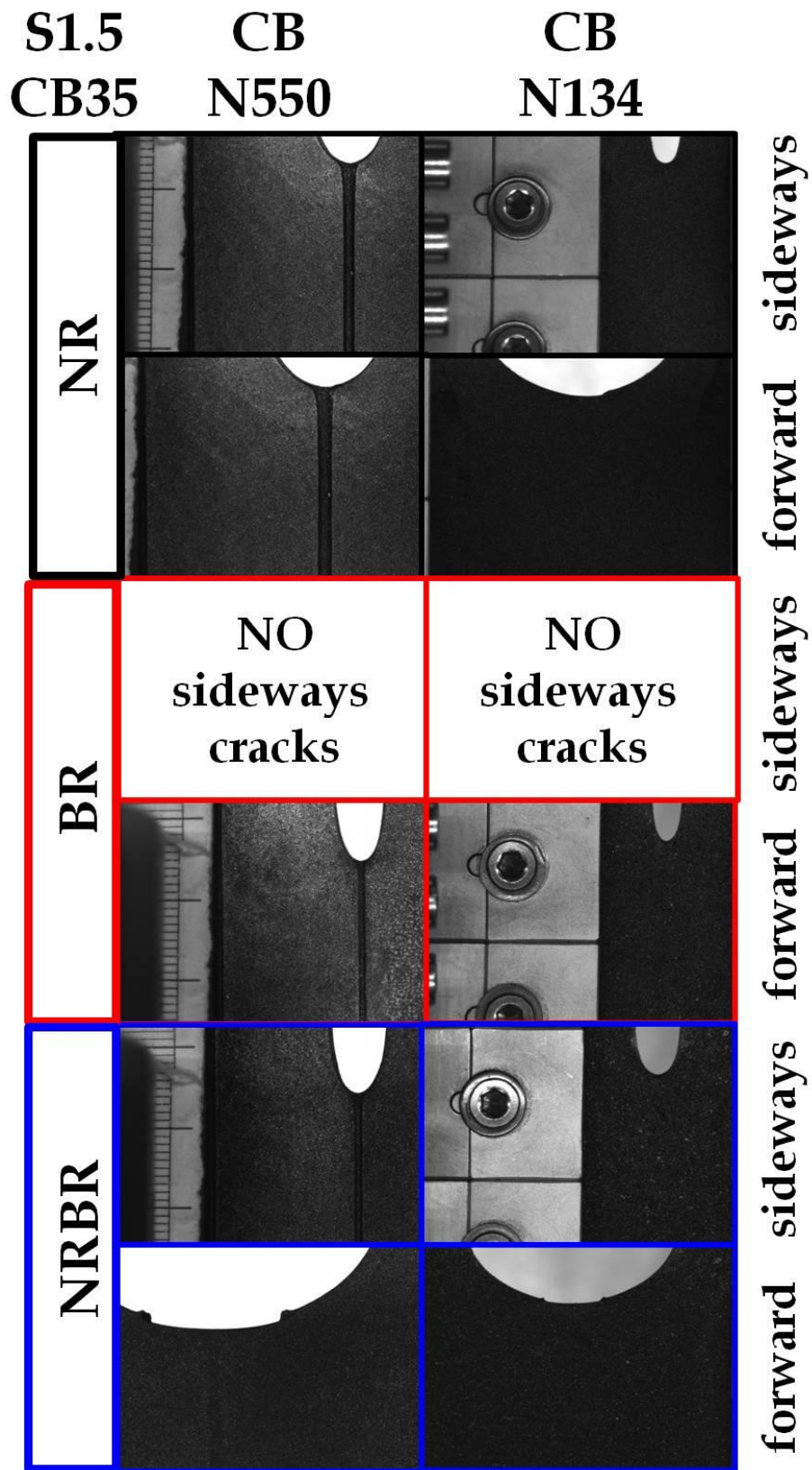


figure 3.31: video frames at sideways and forward cracks onset of NR-BR-NRBR/S1.5/CB35 as a function of carbon black surface area

The corresponding data about the fracture toughness in terms of J-integral were shown in figure 3.32. The energy released at sideways cracks initiation for NR and NRBR increases as surface area increases: these results are consistent with the obtained trend regarding the orientability of the molecular chains of these rubbers (figure 3.28). The fracture toughness at forward crack formation increases for natural rubber, while for the blends it strongly decreases.

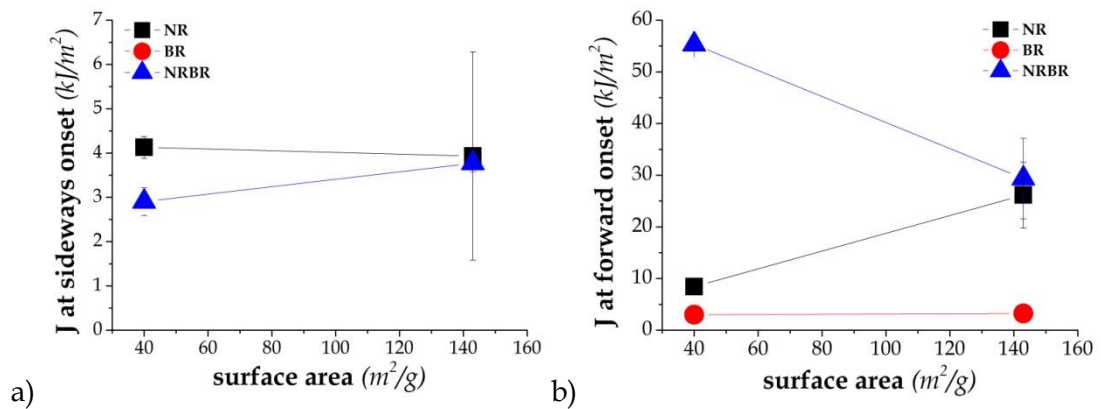


figure 3.32: J at the sideways cracks onset (a) and at forward crack onset (b) of NR-BR-NRBR/S1.5/CB35 as a function of CB surface area

4. Conclusive remarks

A study on the effect of sulfur content, carbon black content and carbon black type was developed on natural rubber, polybutadiene and their 50/50 blend. Some physical characteristics and fracture behavior of these compounds were evaluated and the main findings are here reported.

Regarding the physical characteristics:

- The decrease of the average molecular weight between two junction points, from which crosslink density can be obtained, is the same either by increasing sulfur content from 0.9 phr to 2.1 phr or carbon black from 0 phr to 70 phr (figure 4.1).

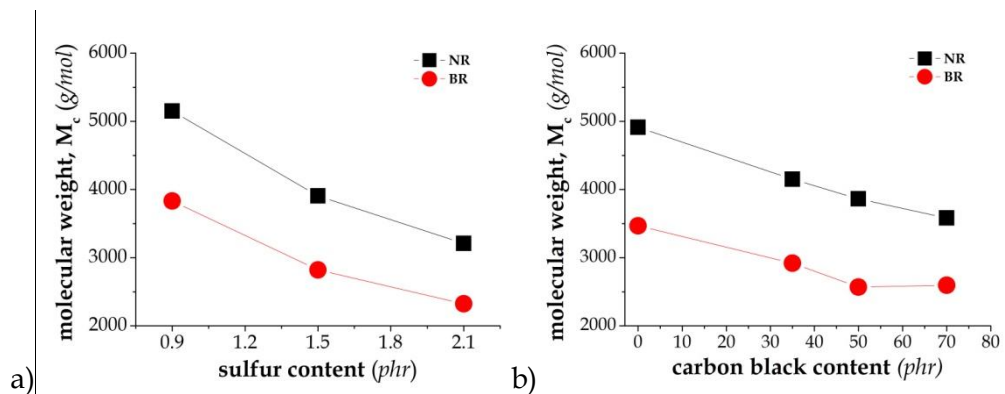


figure 4.1: average molecular weight between two crosslink points, M_c , as a function of sulfur content (a) and carbon black content (b)

- In the compounds examined, the bound rubber is linked mainly to the carbon black content.

This can be deduced from E'_{min} , obtained from dynamic mechanical analysis (DMA), which is determined by the contribution of chemical crosslinking, the hydrodynamic effect of the filler, when present, and the rubber-filler interaction. This latter can be thought as the physical interaction between the rubber and the filler surface (adsorption) and the effects of limited molecular

mobility of part of the rubber (bound rubber). It should be remarked that the crosslink density, obtained from swelling experiments, considers chemical junctions and the junctions between rubber and carbon black irrespective of the “bound rubber”.

From (figure 4.2.a), it can be observed that E'_{min} is practically constant with sulfur content indicating that the range of variation of M_c examined in this work does not significantly affect E'_{min} . Therefore the increase in E'_{min} observed in figure 4.2.b is due to an increase in bound rubber, since the hydrodynamic effect is negligible with respect to the changes observed.

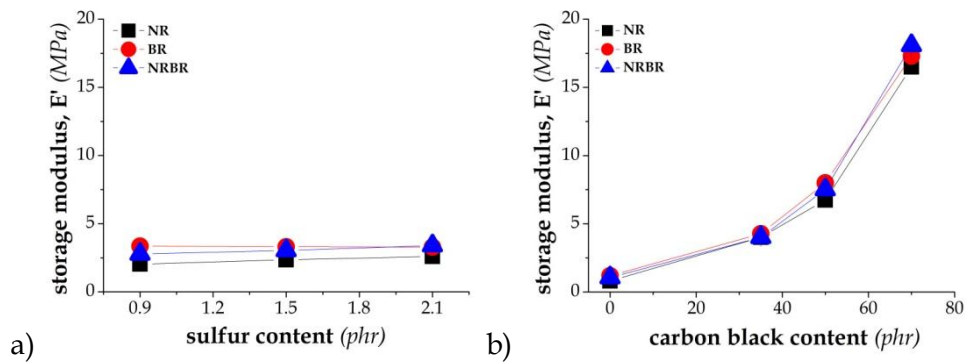
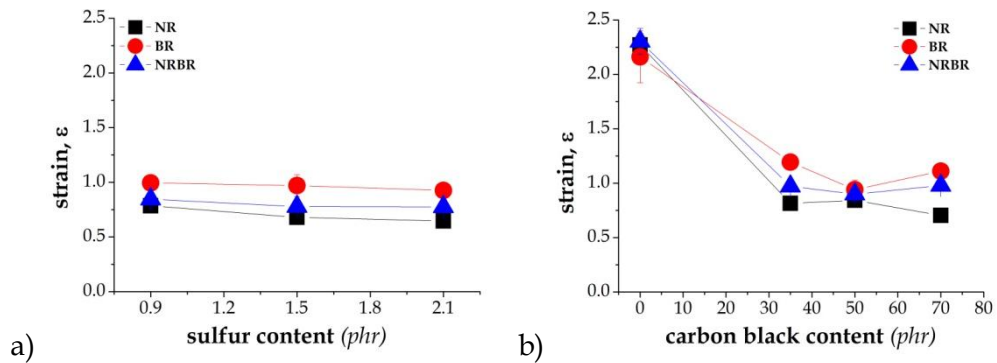


figure 4.2: E'_{min} as a function of sulfur content (a) and carbon black content (b)

- The molecular orientability was related to the maximum chain extension evaluated from the Mooney-Rivlin plot of the data obtained in tensile tests. A large change in maximum chain extension is observed between unfilled and filled compounds. For the filled rubbers the variations in orientability are limited as sulfur content, carbon black content and surface area increase (figure 4.3). Nevertheless, these limited changes could have a significant effect on fracture properties.



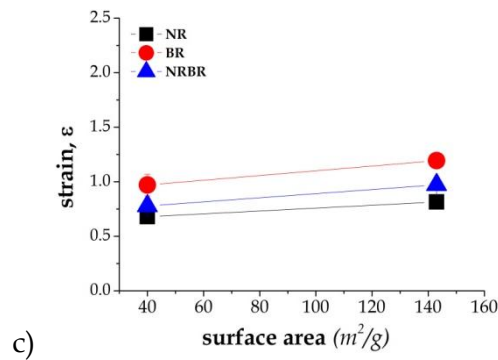


figure 4.3: strain at maximum chain extension as a function of sulfur content (a), carbon black content (b) and surface area (c)

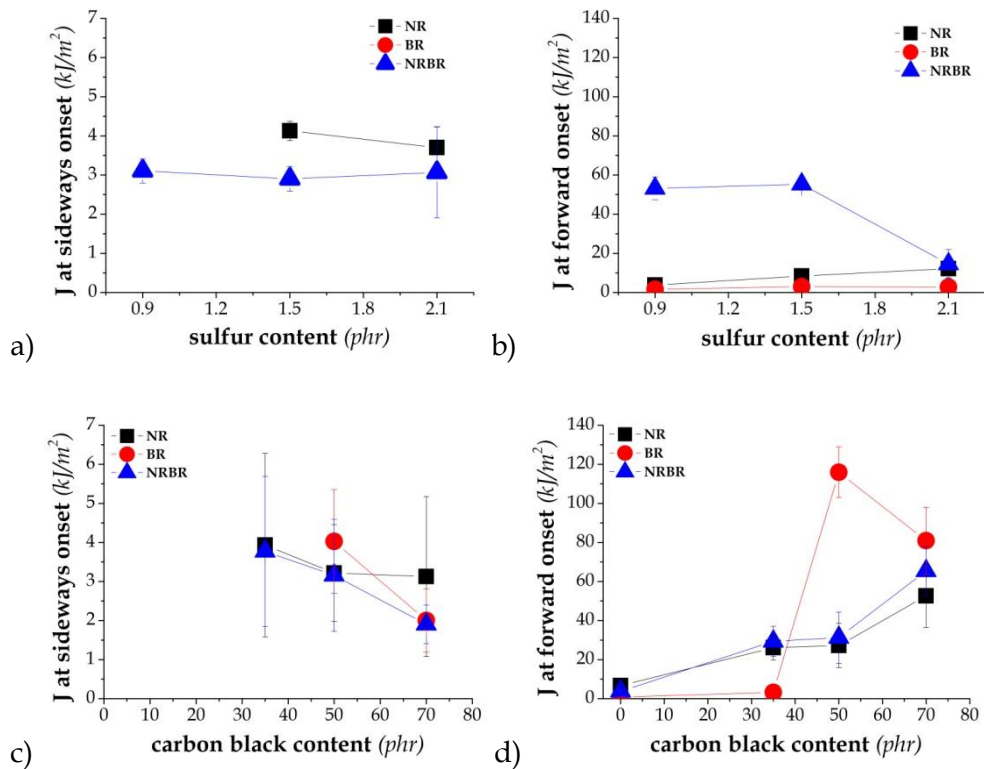
As for fracture behavior (figure 4.4):

- High toughness is observed when sideways cracks develop: before the onset of the “forward” crack along the notched plane of the pure specimen, “sideways” cracks form and propagate perpendicular to the notched plane, thus parallel to the direction of applied load. Nevertheless sideways cracks development is a necessary but not sufficient condition for high fracture toughness. A proper combination of sulfur and carbon black seems to be necessary for the formation of sideways cracks and an optimized fracture toughness depending on the particular rubber matrix.
- Sideways cracks are linked to the orientability of the rubber which generates strength anisotropy. Some correlation between local strains at sideways cracks onset and strain at maximum chain extension in the compounds with different carbon black content (figure 3.19) were found. Fracture toughness at forward crack onset is linked to dissipative deformation mechanisms and reinforcing effects, which may take place at the high strains occurring at the crack tip (see chapter 1 – section 3).
- None of the three unfilled compounds developed sideways cracks, while some of the filled did.
- For filled NR, sideways cracks formed in all compounds except for the one with CB550-35 phr with the lowest sulfur content. Further, the fracture

toughness (J_f) increased as crosslink density, surface area and carbon black content increased.

- For filled BR, sideways cracks developed only for carbon black content above 50 phr, showing the highest J_f among all compounds examined for 50 phr carbon black content. Although for a CB loading of 70 phr J_f was much lower indicating that the relevant dissipative mechanisms can no longer occur.
- In the case of the filled blend, all compounds developed sideways cracks. This is an interesting results since sideways cracks could form even when both relevant neat compounds did not show sideways cracks (NRBR/S0.9/CB550-35).

Then, the blend showed for sulfur content 0.9 and 1.5 phr with CB 35 phr fracture toughness (J_f) values higher than those of both neat compounds (b).



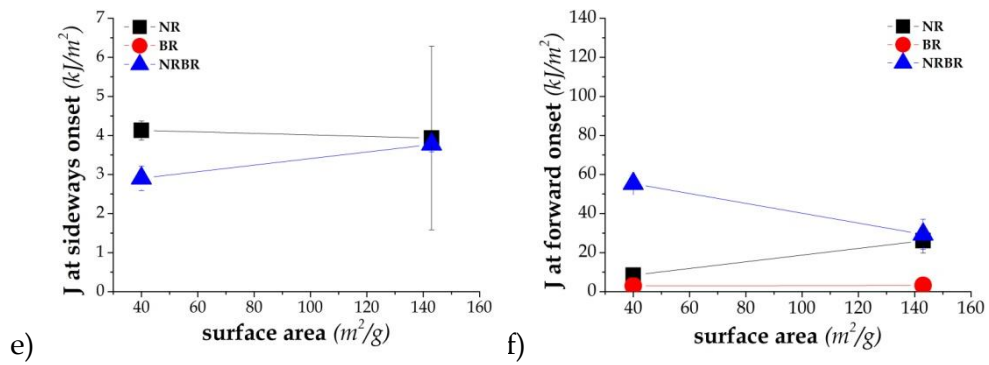


figure 4.4: J at the sideways cracks onset and at forward crack onset of NR, BR, NRBR as a function of sulfur content (a,b), carbon black content (c,d) and surface area (e,f)

Some correlations between the components of the different rubber compounds and both the structural features and the fracture behavior of the compounds were found. Nevertheless the correlation between the latter still needs further investigation.

References

Amnuayporn Sri, S., Toki, S., & Hsiao, B. S. (2012). The effect of endlinking network and entanglements to stress-strain relation and strain-induced crystallization of unvulcanized and vulcanized natural rubber. *Polymer* , 53: 3325-3330.

Boggio, M. (2010). Fracture behavior of carbon black filled natural rubber . *PhD Thesis, Politecnico di Milano: Milano, Italy* .

Bokobza, L. (2001). Reinforcement of elastomeric networks by fillers. *Macromolecular Symposia* , 169: 243-260.

Bokobza, L. (2004). Reinforcement of elastomeric networks by fillers. *Macromolecular materials and engineering* , 289: 607-621.

Bokobza, L., & Chauvin, J. (2005). Reinforcement of natural rubber: use of in situ generated silicas and nanofibres of sepiolite. *Polymer* , 46: 4144-4151.

Calabrò, R. (2013). *PhD Thesis, Politecnico di Milano: Milano, Italy* .

Cazzoni, E., Calabrò, R., Marano, C., & Rink, M. (2013). Mechanical characterization of carbon black filled NR/BR compounds from small strains up to fracture. *ECCMR 2013* .

Chenal, J., Chazeau, & L., G. L. (2007). Molecular weight between physical entanglements in natural rubber: a critical parameter during strain-induced crystallization. *Polymer* , 48: 1042-1046.

Dick, J. S. (2003). *Basic rubber testing: selecting methods for a rubber test program*. ASTM International.

Fetters, L. J., Lohse, D. J., & Colby, R. H. (2006). Chain dimensions and entanglements spacing. *Physical properties of polymers handbook* , 25: 445-452.

- Fröhlich, J., Niedermeier, W., & Luginsland, H.-D. (2005). The effect of filler-filler and filler-elastomer interaction on rubber reinforcement. *Composites: Part A* , 36: 449-460.
- Gent, A. N. (2001). *Engineering with rubber*, Munich, Hanser .
- Gent, A. N., Razzaghi-Kashani, M., & Hamed, G. R. (2003). Why do cracks turn sideways? *Rubber chemistry and technology* , 76: 122-131.
- Hamed, G. R. (1990). Energy dissipation and fracture of rubber vulcanizates. *Rubber chemistry and technology* , 64: 493-500.
- Hamed, G. R. (2001). Materials and Compounds. In A. N. Gent, *Engineering with rubber: how to design rubber components, 2nd edition*. Hanser.
- Hamed, G. R. (1994). Molecular aspects of the fatigue and fracture of rubber. *Rubber chemistry and technology* , 67: 529-536.
- Hertz, D. L. (2001). Introduction. In A. N. Gent, *Engineering with rubber: how to design rubber components, 2nd edition*. Hanser.
- Hocine, A. N., Abdelaziz, N. M., & Imad, A. (2002). *International Journal of Fracture* , 117: 1.
- Leblanc, J. (2000). Elastomer-filler interactions and rheology of filled rubber compounds. *Journal of applied polymer science* , 78: 1541-1550.
- Marano, C., Boggio, M., Cazzoni, E., & Rink, M. (Accepted for publication in press). Fracture phenomenology and toughness of filled natural rubber compounds via the pure shear test-specimen.
- Marano, C., Mohammadpoor, S., & Rink, M. (2013). Characterization of high cis-content polybutadiene compounds differing in cis-content and molecular weight distribution. *ECCMR 2013* .
- Mark, J. E., Erman, E., & Eirich, F. (2005). *The science and technology of rubber, 3rd edition*. Elsevier.

- Shaw, M. T., & MacKnight, W. J. (2005). *Introduction to polymer viscoelasticity*, 3rd edition. Wiley.
- Sircar, A. K., Lamond, T. G., & Pinter, P. E. (1973). Effect of heterogeneous carbon black distribution on the properties of polymer blends. *Meeting of the Rubber Division, ASC, Denver* , 48-56.
- Treolar, L. R. (2005). *The physics of rubber elasticity*, 3rd edition. Clarendon Press Oxford.
- Walters, M., & Keyte, D. N. (1965). Heterogeneous structure in blends of rubber polymers. *Rubber chemistry and technology* , 38: 62-75.
- Wolff, S. M., Wang, J., & Tan, E. H. (1991). Filler-elastomer interactions. Part VII. Study on bound rubber. *Meeting of the Rubber Division ACS, Detroit* , 163-177.
- Wolff, S., & Wang, M. J. (1991). Filler-elastomer interactions. Part IV. The effect of the surface energies of fillers on elastomers reinforcement. *Meeting of the Rubber Division ACS, Toronto* , 329-342.